MESOSCOPIC EFFECTS IN BOSE-EINSTEIN CONDENSATE

FLUCTUATIONS OF AN IDEAL GAS IN A BOX

A Thesis

by

KONSTANTIN DORFMAN

Submitted to the Office of Graduate Studies of
Texas A&M University
in partial fulfillment of the requirements for the degree of

MASTER OF SCIENCE

August 2008

Major Subject: Physics

MESOSCOPIC EFFECTS IN BOSE-EINSTEIN CONDENSATE

FLUCTUATIONS OF AN IDEAL GAS IN A BOX

A Thesis

by

KONSTANTIN DORFMAN

Submitted to the Office of Graduate Studies of
Texas A&M University
in partial fulfillment of the requirements for the degree of

MASTER OF SCIENCE

Approved by:

Chair of Committee,	Vitaly Kocharovsky
Committee Members,	Glenn Agnolet
	Alexey Belyanin
	Peter Kuchment
Head of Department,	Edward Fry

August 2008

Major Subject: Physics

ABSTRACT

Mesoscopic Effects in Bose-Einstein Condensate

Fluctuations of an Ideal Gas in a Box. (August 2008)

Konstantin Dorfman, B.S., Nizhny Novgorod State University

Chair of Advisory Committee: Dr. Vitaly Kocharovsky

The mesoscopic effects in the quantum trapped gases of the Bose atoms consti-
tute the main subject of the present thesis. These effects are the most difficult for
the theoretical analysis in the quantum statistical physics since they can't be seen by
neither a standard quantum mechanics of the simple microscopic systems of one or
very few atoms nor a standard statistical physics of the macroscopic systems that are
infinite in the bulk (thermodynamic) limit.

Most of the experiments on the cold quantum gases performed in the last decade,
starting from the first demonstration of BEC in 1995, involve the mesoscopic systems
of a finite number of atoms. The mesoscopic effects should manifest themselves most
clearly and easily near a critical temperature of BEC; however, they could be observed
also above and below the critical temperature.

Here I study the quantum and thermal fluctuations of the Bose-Einstein conden-
sate (BEC) in a box with the periodic boundary conditions under a particle-number
constraint. The above constraint is the only reason for the BEC and is crucial for the
mesoscopic effects in the BEC fluctuations, especially in the vicinity of the critical
temperature in the Bose gas.

I employ the particle-number conserving operator formalism of Girardeau and
Arnowitt introduced in 1959 to analyze the canonical ensemble fluctuations. I present
analytical formulas and numerical calculations for the central moments of the ground
state occupation fluctuations in an ideal Bose gas in a box with a mesoscopic number

of particles.

I present the analysis of the BEC statistics both on a temperature at a fixed number of particles and on a number of particles at a fixed temperature. Both analyses are valid for the purpose of understanding the important mesoscopic effects near the critical temperature. I emphasize the non-Gaussian nature of the fluctuations.

The presented formalism can be generalized to the case of a weakly interacting Bose gas in a box in the framework of the Bogoliubov approximation. The work in this direction is in progress but is not included in the present thesis.

To my grandparents, Yuri and Galina Bystrovi

ACKNOWLEDGMENTS

I would like to thank everybody who has inspired, encouraged, and helped in this achievement although it is nearly impossible to come up with a complete list. My sincerest apologies for any oversights that I may make in this attempt as I take the risk of omitting those who deserve at least partial credit for this work.

I would like to express my gratitude to my advisor, Dr. Vitaly Kocharovsky, for his guidance and patience. I would like to thank the members of my committee for their endurance and patience. They are Dr. Glenn Agnolet, Dr. Alexey Belyanin, and Dr. Peter Kuchment.

The Physics Department of Texas A&M University is also gratefully acknowledged.

Finally, I wish to thank my parents for their love, encouragement, understanding, and patience.

TABLE OF CONTENTS

LIST OF FIGURES

CHAPTER I

INTRODUCTION: THE PROBLEM OF BEC FLUCTUATIONS AND MESOSCOPIC EFFECTS

A.   Phenomenon of the Bose-Einstein condensation

In 1924-1925 Einstein published two papers [1, 2] where he generalized the work of Bose [3] on the quantum statistics of photons to the case of an ideal gas with a fixed number of atoms. In the second paper he predicted the condensation of atoms to the lowest energy state. It was shown that at high enough temperature the distribution function of atoms in the momentum space for a large box trap is:

$$\bar{n}_p = \left(\exp\left[\frac{\epsilon(p) - \mu}{T} \right] - 1 \right)^{-1}, \qquad T > T_c, \tag{1.1}$$

where $\mu < 0$ is a chemical potential of a gas and $\epsilon(p) = p^2/2m$ is an atomic energy as a function of momentum $\mathbf{p}$. The distribution becomes different below the temperature of the phase transition T_c. Assuming that the degeneracy factor $g = 1$, one has:

$$T_c = 3.31 \frac{\hbar^2}{m} n^{2/3}, \tag{1.2}$$

where n is the number density of the gas. Below the critical temperature the mean number of atoms $\bar{n}_0$ with the zero momentum $\mathbf{p} = 0$ (the condensed atoms) is macroscopically large, that is proportional to the total number of particles N, namely,

$$\bar{n}_0 = N \left[1 - \left(\frac{T}{T_c} \right)^{3/2} \right], \qquad T < T_c. \tag{1.3}$$

The journal model is Physical Review Letters.

The noncondensed atoms with the momentum $\mathbf{p} \neq 0$ are distributed according to Eq. (1.1) with the zero chemical potential $\mu = 0$, i.e.,

$$\bar{n}_p = \left(\exp\left[\frac{\epsilon(p)}{T}\right] - 1 \right)^{-1}, \qquad T < T_c. \tag{1.4}$$

The phenomenon of Bose-Einstein condensation (BEC) plays an important role in many physical systems, including superliquid Helium, electrons in the supercon- ductors, excitons in the semiconductors. In all these cases BEC is mixed with a strong interaction or a complicated structure of the system itself. For example, there is no doubt, that the condensate exists in the superliquid ^{4}He, but the precise measurement of the number of condensed atoms from the neutron scattering data is not direct and involves complicated theoretical calculations.

The problem of BEC is related to the theory of superfluidity and the phenomenon of second order phase transition. Following the classical Landau theory of the second order phase transitions applied to the liquid Helium [4, 5], one can conclude that the occurence of superfluidity in liquid helium involves a second order phase transition, which results in the qualitative change in the properties of the matter. From the microscopic point of view, the transition between the normal state and the superfluid state at the λ-point depends on the certain property of the momentum distribution of the actual particles; namely in a superfluid, a macroscopically large number of particles have zero momentum, which means that these particles form Bose-Einstein condensate in the momentum space.

The theory of BEC is formulated in terms of the $\hat{\Psi}$ operator, which can be written in the Heisenberg representation as follows:

$$\hat{\Psi}(\mathbf{r}, t) = \frac{1}{\sqrt{V}} \sum_{\mathbf{p}} \hat{a}_{\mathbf{p}} \exp\{\frac{i}{\hbar}\mathbf{p} \cdot \mathbf{r} - \frac{i}{\hbar}\frac{p^2}{2m}t\}. \tag{1.5}$$

Ignoring the non-commutativity of the operators $\hat{a}_0$ and $\hat{a}_0^\dagger$, one can write the $\hat{\Psi}$ operator as:

$$\hat{\Psi} = \hat{\Xi} + \hat{\Psi}', \qquad \hat{\Psi}^\dagger = \hat{\Xi}^\dagger + \hat{\Psi}'^\dagger, \tag{1.6}$$

where the operators $\Xi^\dagger$ and Ξ are the creation and annihilation operators of the particle in the condensate. In the thermodynamic limit, i.e. at $N \to \infty$, $V \to \infty$ and a finite given value of the number density N/V, the matrix elements of the Ξ operators can be written as:

$$\lim_{N\to\infty} \langle m, N|\hat{\Xi}|m, N+1\rangle = \Xi, \qquad \lim_{N\to\infty} \langle m, N+1|\hat{\Xi}^\dagger|m, N\rangle = \Xi^*, \tag{1.7}$$

where Ξ is a complex number. Since the remaining part, corresponding to the non-condensate, converts the state $|m, N\rangle$ into states orthogonal to it, one has zero matrix elements

$$\lim_{N\to\infty} \langle m, N|\hat{\Psi}'|m, N+1\rangle = \lim_{N\to\infty} \langle m, N+1|\hat{\Psi}'^\dagger|m, N\rangle = 0 \tag{1.8}$$

and in the thermodynamic limit the difference between states $|m, N\rangle$ and $|m, N+1\rangle$ disappears entirely. In this sense, the quantity Ξ becomes the mean value of the operator $\hat{\Psi}$ for that state.

In the homogeneous liquid at rest, the quantity Ξ is independent of the coordinates and time, which can be proved by the appropriate choice of the phase of this complex quantity and by considering the Hamiltonian $\hat{H}' = \hat{H} - \mu\hat{N}$. Therefore,

$$\Xi = \sqrt{\bar{n}_0}, \tag{1.9}$$

where $\bar{n}_0$ is the mean number of the condensate particles per unit volume of the liquid. In the case of the superfluid motion, which takes place in the liquid under the non-stationary and non-uniform (over distances large in comparison with the interatomic distances) external conditions, the BEC occurs, but now one cannot assert that it

will occur in the state with the zero momentum. The quantity Ξ, defined in Eq. (1.7), now is the function of the coordinates and time and represents the particle wavefunction in the condensate state. It is normalized by the condition $|\Xi|^2 = \bar{n}_0$, and can, therefore, be expressed as:

$$\Xi(t, \mathbf{r}) = \sqrt{\bar{n}_0(t, \mathbf{r})} \exp(-i\Phi(t, \mathbf{r})). \tag{1.10}$$

The gradient of the phase of the condensate wavefunction determines the velocity of the superflluid motion

$$\mathbf{v}_s = (\hbar/m)\nabla\Phi. \tag{1.11}$$

Since there is a macroscopically large number of particles in the condensate, the wave function of this state becomes a classical macroscopic quantity.

The existence of the condensate changes dramatically the density matrix compare to the ordinary liquid, which is given by:

$$N\rho(\mathbf{r_1}, \mathbf{r_2}) = \langle m, N|\hat{\Psi}^\dagger(t, \mathbf{r_2})\hat{\Psi}(t, \mathbf{r_1})|m, N\rangle. \tag{1.12}$$

In the homogeneous liquid, this function depends only on the difference $\mathbf{r} = \mathbf{r_1} - \mathbf{r_2}$. Therefore, substituting the operator $\hat{\Psi}$ from the Eq. (1.6) and using the properties of Eqs. (1.7) and (1.8), we get:

$$N\rho(\mathbf{r_1}, \mathbf{r_2}) = \bar{n}_0 + N\rho'(\mathbf{r_1}, \mathbf{r_2}). \tag{1.13}$$

The density matrix ρ' for the noncondensed particles tends to zero as $|\mathbf{r_1} - \mathbf{r_2}| \to \infty$, whereas the total density matrix ρ tends to the finite limit $\bar{n}_0/N$. This expresses the "long-range order" in a superfluid, which is not present in ordinary liquids, where one always has $\rho \to 0$ as $|\mathbf{r_1} - \mathbf{r_2}| \to \infty$. The fact that Ξ is complex, means that the order parameter, which characterizes the symmetry of the system, has two components, and

the effective Hamiltonian [4] of the system depends only on $|\Xi|^2$, i.e. is invariant under the transformation $\Xi \to e^{i\alpha}\Xi$ for any real phase α.

The empirical results concerning the λ-transition in liquid helium, seem to indicate, that there is no region in which the Landau theory of phase transitions [4-6] is valid, since $|T - T_\lambda| << T_\lambda$. Hence, one should employ the fluctuation theory of the phase transitions of the second kind to relate the temperature dependences of various quantities. In particular, the temperature dependence of the order parameter and, therefore, the condensate density $\bar{n}_0$ as $T \to T_\lambda$ is given by the critical index β [4, 6],

$$|\Xi| = \sqrt{\bar{n}_0} \propto (T_\lambda - T)^\beta. \tag{1.14}$$

The temperature dependence of the specific heat c_p is of special interest. In the following discussion, I will show that it is related to the superfluid density. One can employ the hypothesis of the scale invariance, which implies, that the characteristic length of the fluctuations is the correlation radius r_c of the fluctuations. Thus, the square of the superfluid velocity, obtained from Eq. (1.11) varies with temperature according to:

$$v_s^2 \propto 1/r_c^2 \propto (T_\lambda - T)^{2\nu}, \tag{1.15}$$

where ν is the critical index of the correlation radius. Considering the long-wavelength fluctuations, which in fact govern the singularity of the thermodynamic quantities at the transition point, one can assume that the kinetic energy close to the transition point varies with the temperature in the same way as the singular part of the thermodynamic potential of the liquid, i.e. as $(T_\lambda - T)^{2-\alpha}$, where α is the critical index of the specific heat c_p. Thus, we find:

$$\rho_s v_s^2 \propto \rho_s (T_\lambda - T)^{2\nu} \propto (T_\lambda - T)^{2-\alpha}, \tag{1.16}$$

whence $\rho_s \propto (T_\lambda - T)^{2-\alpha-2\nu}$. Using the relation $3\nu = 2 - \alpha$ which follows from the hypothesis of scale invariance [4, 6], we have:

$$\rho_s \propto (T_\lambda - T)^{(2-\alpha)/3}, \tag{1.17}$$

which finally relates the temperature dependences of ρ_s and specific heat c_p near the phase transition point.

In order to derive the equation for the condensate wavefunction (order parameter) $\Xi(\mathbf{r}, t)$, one has to write the time evolution of the field operator $\hat{\Psi}(\mathbf{r}, t)$ using the Heisenberg equation of motion with the many-body Hamiltonian [7, 8]:

$$i\hbar\frac{\partial}{\partial t}\hat{\Psi}(\mathbf{r}, t) = \left[\hat{\Psi}, \hat{H}\right] = \left[-\frac{\hbar^2\nabla^2}{2m} + V_{ext}(\mathbf{r}) + \int d\mathbf{r}'\hat{\Psi}^\dagger(\mathbf{r}', t)V(\mathbf{r} - \mathbf{r}')\hat{\Psi}(\mathbf{r}', t)\right]\hat{\Psi}(\mathbf{r}, t), \tag{1.18}$$

where $\hat{H}$ is a many-body Hamiltonian

$$\hat{H} = \int d\mathbf{r}\hat{\Psi}^\dagger(\mathbf{r})\left[-\frac{\hbar^2\nabla^2}{2m} + V_{ext}(\mathbf{r})\right]\hat{\Psi}(\mathbf{r}) + \frac{1}{2}\int d\mathbf{r}d\mathbf{r}'\hat{\Psi}^\dagger(\mathbf{r})\hat{\Psi}^\dagger(\mathbf{r}')V(\mathbf{r} - \mathbf{r}')\hat{\Psi}(\mathbf{r}')\hat{\Psi}(\mathbf{r}). \tag{1.19}$$

Replacing the operator $\hat{\Psi}$ with the classical field Ξ and thus, considering only large distances $\mathbf{r} - \mathbf{r}'$, one can specify the interaction term in Eq. (1.18) in the simplest approximation. Assume that the gas of atoms is cold and dilute, and therefore, only binary collisions at low energy are relevant. These collisions are characterized by a single parameter, the s-wave scattering length a, independently of the details of the two-body potential. Thus, one can replace the interaction term $V(\mathbf{r} - \mathbf{r}')$ in Eq. (1.18) with the following expression:

$$V(\mathbf{r} - \mathbf{r}') = g\delta(\mathbf{r} - \mathbf{r}'), \tag{1.20}$$

where the coupling constant g is related to the scattering length a as follows:

$$g = \frac{4\pi\hbar^2 a}{m}. \tag{1.21}$$

The introduced above interaction term yields to the following equation of motion for the order parameter Ξ:

$$i\hbar\frac{\partial}{\partial t}\Xi(\mathbf{r},t) = \left[-\frac{\hbar^2\nabla^2}{2m} + V_{ext}(\mathbf{r}) + g|\Xi(\mathbf{r},t)|^2\right]\Xi(\mathbf{r},t), \tag{1.22}$$

The Eq. (1.22) is known as Gross-Pitaevskii (GP) equation. It is valid when the s-wave scattering length is much smaller than the average distance between atoms $a << (N/V)^{-1/3}$ (the criteria of dilute gas), and the mean number of atoms in the condensate is large, $\bar{n}_0 >> 1$. The GP equation can be used at low temperature, to explore the macroscopic behavior of the system, characterized by variations of the order parameter over distances larger than the mean distance between atoms.

The experimental systems are the collections of individual neutral alkali-gas atoms, with a total number N ranging from a few hundred up to $\sim 10^{10}$, confined by magnetic and/or optical means to a relatively small region of space. The achieved densities range from $\sim 10^{11} cm^{-3}$ to $\sim 5\times 10^{15} cm^{-3}$ with a temperature, in the region of interest, typically in the range between a few tens of nK and a few tens of μK.

An alkali atom in its ground state has a single valence electron in an ns^1 state outside one or more closed shells. Therefore the electronic state is a doublet. The only excited state that we are interested in is a np, since it is more favorable to this state to couple to the ground state in the sense of the radiation in optical regime. The wavelength λ of the transition $ns \rightarrow np^1$ lies in the range $5000-7000$ A° and the excited state lifetime is 20 nsec. Since for the alkali atoms the atomic number Z is odd, it means that for odd isotopic number A, the systems such as ^{87}Rb, ^{23}Na, ^7Li will obey the Bose-Einstein statistics, whereas an even-A systems such as ^6Li or ^{40}K

will obey Fermi-Dirac statistics.

It is important to outline the general features of the resulting effective potentials in which the atoms move, i.e. the trapping potentials. There are two types of trapping potentials which are widely used in the experiments. The first type is based on the atom-laser interaction. The effect that has been principally exploited in the laser trapping of atoms in BEC regime is the so-called dipole effect, which relies on the interaction of the laser field with the electric dipole moment which is induced in the atom. One can define the detuning of the $ns \rightarrow np$ transition frequency as:

$$\Delta = \hbar\omega_{las} - (\epsilon_{np} - \epsilon_{ns}) \equiv \hbar\omega_{las} - 2\pi\hbar c/\lambda. \qquad (1.23)$$

The energy change in the atom is inverse proportional to the detuning Δ. A region of high laser intensity, thus, provides an attractive potential for $\Delta < 0$ ("red detuning") and a repulsive potential $\Delta > 0$ ("blue detuning"). However, there are different problems concerning this type of confinement such as sensitivity to the hyperfine-Zeeman splitting, the spontaneous emission, etc. which I do not discuss here.

The second type of the trap potential arises from the magnetic analogue of the Earnshaw theorem, which forbids the magnitude of the magnetic field $\mathbf{B}(\mathbf{r})$ to have a local maximum in free space. However, nothing forbids the occurrence of the local minimum, which can be provided by various methods. Virtually all non-laser assisted magnetic traps used in BEC experiments to date have had axial symmetry and a finite offset field, thus, it can be written in cylindrical coordinates as:

$$|\mathbf{B}(\mathbf{r})| = B_0 + \frac{1}{2}\alpha\rho^2 + \frac{1}{2}\beta z^2. \qquad (1.24)$$

The cooling process usually consists of two steps. First, the laser cooling technique is used. Then, the atoms are evaporated from the trap. Since particles with higher energies are evaporating faster than the ones with lower energies, the process of

evaporation leads to the cooling. The temperature obtained in the described process can be of the order of hundreds of nK and allows one to observe the condensate. The most recently developed experimental techniques dropped the temperature to several nK.

In gases, BEC was observed only in 1995, namely, in the vapor alkali gases using the advanced experimental setup [9–12]. I will present the typical experiment parameters based on the two pioneering papers [9, 10]. In the first experiment, BEC was produced in a vapor of rubidium-87 atoms [9] that was confined by magnetic field and evaporatively cooled. Six laser beams intersect in a glass cell creating a magneto-optical trap. The cell was 2.5 cm square by 12 cm long, and the beams were 1.6 cm in diameter. The condensate fraction first appeared near the temperature of 170 nK at a number density of 2.5×10^{12} atoms per cubic centimeter and could be preserved for more than 15 seconds. The s-wave scattering length was about 10^{-6} cm. In another pioneering experiment [10] the BEC was observed in the gas of sodium atoms, which were confined in a novel trap that employed both magnetic and optical forces. Evaporative cooling increased the phase-space density by 6 orders of magnitude within 7 seconds. Condensates contained up to 5×10^5 atoms at densities exceeding 10^{14} cm^{-3}. The critical temperature for the experiment was 2 μK. The trapping volume was of the order of $10^{-8} cm$. The corresponding scattering length of the sodium atoms was 4.9 nm.

The described experimental setups later allowed one to measure directly the number statistics in a Bose gas [13, 14]. It can be done in the following way. For number of order 10^3 or larger, absorption imaging is used yielding spatial and number information. At lower atom numbers, however, fluorescence imaging is used, because of higher signal-to-noise ratio in this regime. This is accomplished by transferring the atoms into a small magneto-optical trap (MOT). This transfer shows the saturation

behavior with MOT beam intensity, indicating that all atoms are captured. The resulting fluorescence signal is detected by a charge-coupled-device (CCD) camera and is properly calibrated. Because of low density during exposure, there is little possibility for multiple scattering events during detection. Therefore, the measured fluorescence signal from the MOT is proportional to the number of atoms present.

The phenomenon of BEC can be observed not only in a harmonic trap [9–11], but in a box as well [15]. In the latter case the axial motion of the rubidium-87 atoms was confined by optical endcaps, producing the "textbook geometry" of a "particle in a box". The resulting atomic number in this box was generally from 500 to 3500 and was controlled by evaporation timing and spacing of the endcaps. The characteristic size of the box was 18 μm, scattering length was 5.6 nm.

The BEC has a lot of applications. The rapid progress in the quantum-coherent manipulation of mesoscopic cold atom clouds results in the construction of the permanent magnet atom chips. Small-scale magnetic field patterns for atom chips can be made using either microfabricated curent-carrying wires or microscopic structures of permanent magnetization. The second idea is less realistic since there is no power dissipation in a permanent magnet. Therefore, a long thin BEC can be prepared in a microtrap formed by a videotape atom chip and can be manipulated in the waveguides of the chip [16]. Moreover, the same effects were used to construct the atomic Michelson interferometer [17]. In this case the splitting, reflecting and recombining of condensate was achieved by a standing wave field. The differential phase shift between two arms of the interferometer was introduced either by the magnetic-field gradient or the initial velocity of condensate. The phase coherence effect between two spatially separated BECs on the atomic chip was observed in [18], which showed that it is both promising and possible to use condensate at high density for interferometry on an atom chip.

The confined BEC in harmonic trap can be also used to realize a quantum gyroscope [19] characterized by two important superfluid effects: the reduced value of the inertia of the sample and the quantization of the angular momentum associated with the vortex. Theoretically proposed gyroscope [19] was characterized by the precession of the symmetry axis of the condensate around the symmetry axis of the confining trap.

Concluding the general introduction, I can state that not only the Einstein's prediction was correct, but the existence of the new type of matter was discovered, where the quantum effects play the leading role at the macroscopic and mesoscopic scale. This phenomena has a lot of applications and connections to the different physical effects of quantum and statistical mechanics and thermodynamics.

B. Theoretical models of BEC quantum statistics

1. Standard theory of BEC and the problem of the mesoscopic effects

Inspired by the series of papers [20, 21], in this dissertation I will try to further develop the quantum statistical theory of BEC fluctuations. In this work I will be mostly focus on the mesoscopic effects, i.e. effects which arise from the fact that the number of atoms in the trap is finite and cannot be represented by an infinite thermodynamic limit. In this chapter I review the existing in the literature understanding of the problem of the BEC fluctuations. The difficulty in the description of the mesoscopic effects is that there is no certain approach for tackling the problem in the standard quantum mechanical theory of the microscopic systems of very few atoms. On the other hand, the statistical mechanics cannot be applied either, because it deals with the macroscopic systems in the thermodynamic limit.

As it was discussed in the previous section, the recent experimental data [9-11,

12-15] was obtained for the mesoscopic systems of a finite number of particles (from few hundreds to few millions). Therefore, the manifestation of the mesoscopic effects which are clearly seen in the region close to the critical temperature of BEC, should add the experimental and theoretical understanding to the problem of transition between few-body systems to macroscopic systems.

The current study of the mesoscopic effects is dealing with the behavior of the quantum fluctuations of the BEC in a box with the periodic boundary conditions. The particle-number constraint which requires exact conservation of particles in the trap is essentially the reason of the mesoscopic effects near the critical temperature and is a crucial issue of this work.

Historically the previous efforts were mostly dealing with the mean value $\bar{n}_0$ and variance $\langle (n_0 - \bar{n}_0)^2 \rangle$ of the condensed atoms. It was assumed that the condensate fluctuations are almost Gaussian, and higher cumulants (semi-invariants) vanish. In fact it is not true even in the thermodynamic limit that was shown in [21].

Presented in Eq. (1.19) many-body Hamiltonian is describing N weakly interacting via the two-body interatomic potential $V(\mathbf{r} - \mathbf{r}')$ bosons confined by an external potential V_{ext}. It also reflects the processes of annihilation and creation of a particle at the position $\mathbf{r}$ by the field operators $\hat{\Psi}(\mathbf{r})$ and $\hat{\Psi}^\dagger(\mathbf{r})$, respectively. Starting from this Hamiltonian, one can derive the thermodynamic properties of the system, as well as its ground state energy eigenvalue. The Monte-Carlo path-integral method of calculating the thermodynamic properties of the system interacting within a repulsive "hard-sphere" potential gives the exact result within statistical errors, but is impractical for the systems with large number of atoms.

Mean-field approaches are commonly developed for interacting systems in order to overcome the problem of solving exactly the full many-body Schroedinger equation. Apart from the convenience of avoiding heavy numerical work, the mean-field theories

allow one to understand the behavior of a system in terms of a set of parameters having a clear physical meaning. This is particularly true in the case of trapped bosons. Actually, most of the results reviewed in this work show that the mean-field approach is very effective in providing qualitative predictions for the static, dynamic, and thermodynamic properties of these trapped gases. The basic idea for a mean-field description of a dilute Bose gas was formulated by Bogoliubov [5-8, 22, 23]. The main idea is in separating the condensate contribution to the bosonic field operator. In general, the field operator can be written as $\hat{\Psi}(\mathbf{r}) = \sum_k \Psi_k(\mathbf{r})\hat{a}_k$, where $\Psi_k(\mathbf{r})$ are single-particle wave functions and $\hat{a}_k$ are the corresponding annihilation operators. The bosonic creation and annihilation operators $\hat{a}_k^\dagger$ and $\hat{a}_k$ are defined in the Fock space through the relations:

$$\hat{a}_k^\dagger |n_0, n_1, ..., n_k, ...\rangle = \sqrt{n_k + 1}|n_0, n_1, ..., n_k + 1, ...\rangle,$$

$$\hat{a}_k |n_0, n_1, ..., n_k, ...\rangle = \sqrt{n_k}|n_0, n_1, ..., n_k - 1, ...\rangle, \qquad (1.25)$$

where n_k are the eigenvalues of the operator $\hat{n}_k = \hat{a}_k^\dagger \hat{a}_k$ giving the number of atoms in the single-particle state. They obey the usual commutation relationships:

$$[\hat{a}_p, \hat{a}_k^\dagger] = \delta_{p,k}, \qquad [\hat{a}_k, \hat{a}_p] = 0, \qquad [\hat{a}_p^\dagger, \hat{a}_k^\dagger] = 0. \qquad (1.26)$$

BEC occurs when the mean number of atoms $\bar{n}_0$ of a particular single-particle state becomes very large: $\bar{n}_0 >> 1$ and the ratio $\bar{n}_0/N$ remains finite in the thermodynamic limit $N \to \infty$. In this limit the states with $\bar{n}_0$ and $\bar{n}_0 \pm 1 \approx \bar{n}_0$ correspond to the same physical configuration and, consequently, the operators $\hat{a}_0$ and $\hat{a}_0^\dagger$ can be treated like c numbers: $\hat{a}_0 = \hat{a}_0^\dagger = \sqrt{\bar{n}_0}$. Therefore, the Hamiltonian in Eq. (1.19) can be written

in the momentum representation as following:

$$H = \sum_{\mathbf{k}} \frac{\hbar^2 \mathbf{k}^2}{2m} \hat{a}_{\mathbf{k}}^{\dagger} \hat{a}_{\mathbf{k}} + H_{int}, \tag{1.27}$$

where the interaction part of the Hamiltonian is approximated as:

$$H_{int} = \frac{g}{2V} \left[\hat{n}_0^2 + 2\hat{n}_0 \sum_{\mathbf{k} \neq 0} (\hat{a}_{-\mathbf{k}}^{\dagger} \hat{a}_{-\mathbf{k}} + \hat{a}_{\mathbf{k}}^{\dagger} \hat{a}_{\mathbf{k}}) + \hat{n}_0 \sum_{\mathbf{k} \neq 0} (\hat{a}_{\mathbf{k}}^{\dagger} \hat{a}_{-\mathbf{k}}^{\dagger} + \hat{a}_{\mathbf{k}} \hat{a}_{-\mathbf{k}}) \right], \tag{1.28}$$

where g is the interaction strength in Eq. (1.21). The total number of particles in the system is:

$$N = \hat{n}_0 + \frac{1}{2} \sum_{\mathbf{k} \neq 0} (\hat{a}_{-\mathbf{k}}^{\dagger} \hat{a}_{-\mathbf{k}} + \hat{a}_{\mathbf{k}}^{\dagger} \hat{a}_{\mathbf{k}}). \tag{1.29}$$

Considering Bogoliubov canonical transformation of the creation and annihilation operators, which diagonalizes the Hamiltonian in Eq. (1.28)

$$\hat{a}_{\mathbf{k}} = \frac{1}{\sqrt{1 - A_{\mathbf{k}}^2}} \left(\hat{\alpha}_{\mathbf{k}} + A_{\mathbf{k}} \hat{\alpha}_{-\mathbf{k}}^{\dagger} \right), \qquad \hat{a}_{\mathbf{k}}^{\dagger} = \frac{1}{\sqrt{1 - A_{\mathbf{k}}^2}} \left(\hat{\alpha}_{\mathbf{k}}^{\dagger} + A_{\mathbf{k}} \hat{\alpha}_{-\mathbf{k}} \right). \tag{1.30}$$

In new operator basis $\hat{\alpha}_{\mathbf{k}}$ and $\hat{\alpha}_{\mathbf{k}}^{\dagger}$, the Hamiltonian looks like:

$$H = E_0 + \sum_{\mathbf{k} \neq 0} \epsilon_{\mathbf{k}} \hat{\alpha}_{\mathbf{k}}^{\dagger} \hat{\alpha}_{\mathbf{k}}, \tag{1.31}$$

with the modified spectrum

$$\epsilon_{\mathbf{k}} = \sqrt{\left(\frac{\hbar^2 \mathbf{k}^2}{2m} + \frac{g \bar{n}_0}{V} \right)^2 - \left(\frac{g \bar{n}_0}{V} \right)^2}, \tag{1.32}$$

and parameters

$$E_0 = \frac{g N^2}{2V}, \qquad A_{\mathbf{k}} = \frac{V}{g \bar{n}_0} \left(\epsilon_{\mathbf{k}} - \frac{\hbar^2 \mathbf{k}^2}{2m} - \frac{g \bar{n}_0}{V} \right). \tag{1.33}$$

The result of the original Bogoliubov calculation was that only small fraction of the atoms were removed from the condensate at $T = 0$ due to a weak interaction.

Specifically, the mean number of particles in the condensate:

$$\bar{n}_0 = N \left(1 - \frac{8}{2} \left(\frac{a^3 N}{\pi V} \right)^{1/2} \right), \tag{1.34}$$

where a is the s-wave scattering length. For a dilute Bose gas, we have $(N/V)a^3 << 1$. In spite of this small interaction-induced depletion, the Bogoliubov model shows that the interactions in the presence of a condensate lead to an acoustic (or phonon) excitation spectrum at long-wavelengths. More precisely, in the limit of small momentum the energy in Eq. (1.32) becomes linear in momentum:

$$\epsilon_{\mathbf{k}} \approx \hbar c k, \tag{1.35}$$

with the phonon velocity $c = (4\pi\hbar^2 a/m(N/mV))^{1/2}$. For the large momentum the Bogoliubov spectrum becomes the free particle spectrum:

$$\epsilon_{\mathbf{k}} \approx \frac{\hbar^2 \mathbf{k}^2}{2m}, \tag{1.36}$$

which agrees with Landau theory of superfluidity [4].

In the presented above Bogoliubov prescription, the condensate acts like a classical particle reservoir, which the noncondensate atoms can enter and leave via scattering. Thus, the number of atoms is no longer a constant of motion. As an immediate consequence, one needs to include anomalous propagators (Green's functions) representing two particles going into or out of the condensate. This approach forms the basis of the systematic application of the quantum field theory to an interacting system of bosons due to Beliaev [7, 8, 22]. This leads to a generalized Green's function formalism which builds in the crucial role of the Bose condensate, and allows one to determine the general characteristics of the system, such as the excitation spectrum, the momentum distribution of atoms, etc. After this pioneer work, this field of study has been extensively developed and extended (for a review, see Ref. [8]).

In principle, one can calculate the properties of an interacting Bose system, such as thermodynamic potential, specific heat, condensate density, etc. As at $T = 0$, such finite T calculations are complicated by the subtle role of correlations induced by the Bose-broken symmetry. Moreover, even in a dilute gas, the finite T case is difficult because the thermally induced depletion fraction is now large. One has to be careful in treating the condensate and excited atoms in a consistent fashion. Another well-known difficulty is the fact that even for regular repulsive interactions, perturbation theory for Bose-condensed systems diverges at small momenta [8, 22]. That is to say, certain terms in the perturbation series are singular for $\mathbf{k} \to 0$, a result which can be traced back to the fact that the single-particle excitations are phonon-like. These singularities have to be handled with care in order to obtain correct final results. Fortunately, the infrared divergences appear to cancel out in all physical quantities [8].

2. Microcanonical, canonical and grand-canonical statistics

Specific experimental conditions define which statistics should be applied in a given particular situation. In view of the present experiments on the trapped atoms of dilute gases, dealing with a finite and well defined number of particles, the most important descriptions are due to the microcanonical and canonical ensembles, since the particle number, even if it is not know exactly, certainly does not fluctuate after the cooling process is over. Magnetic and optical confinement also implies that the system is thermally isolated, which restricts one to the consideration of the microcanonical ensemble. In the other way of cooling, so called the sympathetic cooling, which takes place in the systems of mixed Bose-Fermi gases or Bose gases with different components, there is an exchange of energy between different species of the gas, and thus the canonical ensemble is much more appropriate. This description is appropriate

also for the dilute ^{4}He in a porous medium [24–26]. In the canonical ensemble only the total number of particles is constrained to be conserved $\hat{N} = const$, but energy $\hat{H}$ has non-zero fluctuations and only its average value is a constant $\langle \hat{H} \rangle = \bar{H} = E = const$, determined by a fixed temperature of the system T.

The standard textbooks [4, 5, 22, 23] formulate the BEC statistics problem either in a grand-canonical ensemble, allow the system to exchange both energy and particles with a reservoir at a given temperature T and chemical potential μ, which fixes only the average energy and number of particles, respectively, or some restricted ensembles. The purpose of the restricted ensemble is to select only those states, which ensure the condensate wave function to have almost fixed phase and amplitude [5]. Although these formulations avoid the difficulties of operator constraints on the total energy and particle number which are present in the microcanonical and canonical treatments, they provide effective tools for study of the thermodynamic limit and hydrodynamic properties of the many-body Bose system at the expense of the artificial modification of the condensate statistics. In this case even below the Bose-Einstein condensation temperature, where the ground state mean occupation number is macroscopically large in the sense that $\bar{n}_0 \approx N$, the grand-canonical distribution function

$$\rho_\nu^{GC}(n_\nu) = \frac{1}{1 + \bar{n}_\nu} \left(\frac{\bar{n}_\nu}{1 + \bar{n}_\nu} \right)^{n_\nu} \tag{1.37}$$

in the ground state $\rho_0^{GC}(n_0)$ becomes very broad and even at $T \to 0$ the variance is anomalously large $\langle (n_0 - \bar{n}_0)^2 \rangle \approx \bar{n}_0^2 \propto N^2$. This prediction contradicts with the basic fact that at low temperatures all particles are expected to occupy the ground state with no fluctuations left. Thus the grand-canonical ensemble could be misleading if not revised properly. The approach that involves fixation of the phase and amplitude of the condensate wave function is not good for the description of the condensate formation and fluctuations at all.
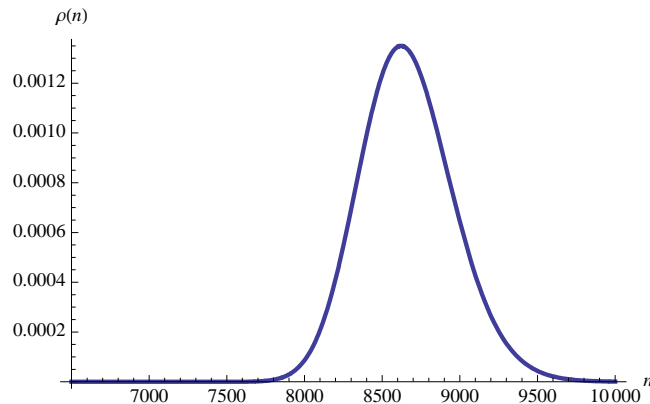
Fig. 1. Negative binomial distribution of the number of noncondensed atoms for an ideal Bose gas in a box with total number of particles $N = 10000$.

It is worthwhile to compare the counting statistics (1.37) with the predictions of other statistics, namely microcanonical and canonical ensembles [5]. For high temperatures $T > T_c$, all three ensembles predict the same behavior. However it is not the same for the low temperature region $T < T_c$. Here the broad grand-canonical distribution function does not agree with the well-peacked canonical and microcanonical distribution function $\rho_0(n_0)$ around the condensate mean occupation number value. In order to illustrate an actual distribution function, I plot in Fig. 1 the finite negative binomial distribution function of the noncondensate occupation in an ideal Bose gas in the canonical ensemble as is derived within the master-equation approach below in Subsection 4, Eq. (1.53). This is the sharp-peaked statistical distribution which was naively expected for a Bose statistics.

The microcanonical and canonical ensemble formalism do not give the same result in all situations. For different traps the agreement requires additional conditions. For example both ensembles have been found to agree in the large-N (almost thermody-namic limit) case for one-dimensional harmonic trap but to differ in the case of three-dimensional isotropic harmonic trap [21]. More general in the case of d-dimensional

σ-power trap, microcanonical and canonical fluctuations agree in large-N limit when $d/\sigma < 2$ and microcanonical fluctuations become smaller than the canonical ones in the case of $d/\sigma > 2$.

For large enough particle number $N > 10^5$ the calculation of microcanonical partition function $\Omega(E, N)$ becomes very time consuming or even impossible. In this case one can employ the approximation technique based on the saddle-point method which is discussed in details in Chapter IV and is widely used in the statistical physics. In this method one starts from the grand canonical partition function and utilize the saddle-point method for extracting its required canonical and microcanonical parts. Furthermore, the moments of fluctuations are described by the different order derivatives from the resulting counterparts.

Recently, the new type of ensemble was introduce, so called Maxwell's demon ensemble [20]. In this approach the overall system is divided into two parts: condensate part and the excited states, which undergo the particle, not energy, exchange between each other. This ensemble gives an approximate result for the ground state fluctuations both in the microcanonical and canonical ensembles. This approximation can be understood in the framework of the canonical ensemble quasiparticle approach presented in Chapter II. It also implies that the higher statistical moments for a homogeneous Bose gas should take into an account the particle-number constraint even in the thermodynamic limit.

3. Exact recursion relation for the statistics of the number of condensed atoms in an ideal Bose gas

It is worth noting that there is one useful reference result in the theory of BEC fluctuations, namely, an exact recursion relation for the statistics of the number of condensed atoms in an ideal Bose gas. Although it does not give any simple analytical

answer or physical insight into the problem, it can be used for "exact" numerical simulations for traps containing a finite number of atoms. It is very useful as a tool which compares different approximate analytical solutions. The recursion relation for an ideal Bose gas had been known and used by many authors [20, 21, 23, 27]. In the canonical ensemble, the probability to find n_0 particles occupying the single particle ground state is give by:

$$\rho_0(n_0) = \frac{Z_{N-n_0}(T) - Z_{N-n_o-1}(T)}{Z_N(T)}; \qquad Z_{-1} \equiv 1. \qquad (1.38)$$

The recurrence relation for an ideal Bose gas, thus is:

$$Z_N(T) = \frac{1}{N} \sum_{k=1}^{N} Z_1(T/k) Z_{N-k}(T), \qquad Z_1(T) = 1 + \sum_{\nu=0}^{\infty} e^{-\epsilon_\nu/T}, \qquad Z_0(T) = 1, \qquad (1.39)$$

which allows one to numerically evaluate the statistics (1.38). Here ν stands for a set of quantum numbers enumerating a given single particle energy levels ϵ_ν, and the ground-state energy assumed to be $\epsilon_0 = 0$ by convention. I will apply the relation (1.39) for evaluation the statistics of an ideal gas in a box in the following sections, namely in Chapter II, Section C. An important example is the isotropic, three-dimensional harmonic trap, where one has:

$$Z_1(T) = \sum_{n=0}^{\infty} \frac{1}{2}(n+2)(n+1) e^{-n\hbar\omega/k_B T} = \frac{1}{\left(1 - e^{-\hbar\omega/k_B T}\right)^3}, \qquad (1.40)$$

where $\frac{1}{2}(n+2)(n+1)$ is the degeneracy of the level $\epsilon_n = n\hbar\omega$.

There is a similar recurrence relation in the microcanonical ensemble [20]:

$$\Omega(E, N) = \frac{1}{N} \sum_{k=1}^{N} \sum_{\nu=0}^{\infty} \Omega(E - k\epsilon_\nu, N - k), \qquad \Omega(0, N) = 1, \qquad \Omega(E > 0, 0) = 0, \qquad (1.41)$$

where the sum over ν is finite, since for finite $E < 0$ one has $\Omega(E < 0, N) = 0$.

Therefore, the ground state occupation probability in the microcanonical ensemble is:

$$\rho_0^{MC}(n_0) = \frac{\Omega(E, N - n_0) - \Omega(E, N - n_0 - 1)}{\Omega(E, N)}; \qquad \Omega(E, -1) \equiv 1. \qquad (1.42)$$

4. Dynamical master equation approach

Here I outline another approach to the canonical statistics of ideal Bose gases. It was developed in [28] and utilizes a master equation for the condensate in order to find its equilibrium solution. This approach reveals important parallels to the quantum theory of laser and is based on the analogy between a second-order phase transition and laser threshold behavior. The master equation can be simplified in the approximation of detailed balance in the excited states under an assumption that for a given arbitrary number n_0 of atoms in the condensate the remaining $N - n_0$ excited atoms are in an equilibrium state at the prescribed temperature T.

One can consider the cooling of an ideal noninteracting N-atom Bose gas confined inside a trap. The gas is in contact with a thermal reservoir maintained at the temperature T. The most studies have been concerned with the evaluation of the partition function, which is strongly related to the statistics and thermodynamics of the Bose gas. As it was discussed in [28], one can obtain a simple master equation for the density matrix of the Bose gas as it cools towards the ground state via exchanging the heat with a thermal reservoir. The master equation for the distribution function of the condensed bosons p_{n_0} yields

$$\dot{p_{n_0}} = -\kappa\{K_{n_0}(n_0 + 1)p_{n_0} - K_{n_0-1}n_0 p_{n_0-1} + H_{n_0}n_0 p_{n_0} - H_{n_0+1}(n_0 + 1)p_{n_0+1}\}. \quad (1.43)$$

Here κH_{n_0} and κK_{n_0} are the heating and cooling coefficients (which depend upon trap shape, total number of atoms in the trap N and the temperature T) are similar

to the cavity loss and saturated gain parameters in the original laser master equation:

$$K_{n_0} = \sum_{k'>0}(\eta_{k'} + 1)\langle n_{k'}\rangle_{n_0}, \qquad H_{n_0} = \sum_{k'>0}\eta_{k'}(\langle n_{k'}\rangle_{n_0} + 1), \qquad (1.44)$$

where:

$$\eta_k = \frac{1}{\exp(\epsilon_k/T) - 1}, \qquad \langle n_{k'}\rangle_{n_0} = \sum_{\{n_k\}_{n_0}} n_{k'}\frac{p_{n_0,\{n_k\}_{n_0}}}{p_{n_0}}. \qquad (1.45)$$

One can obtain the steady state distribution of the number of atoms condensed to the ground level of the trap from Eq. (1.43), thus the ground state statistics can be determined. The detailed balance condition involving the cooling and the heating coefficients yields the following expression for the number distribution of the condensed atoms:

$$p_{n_0} = p_0 \prod_{i=1}^{n_0} \frac{K_{i-1}}{H_i}, \qquad (1.46)$$

where the partition function

$$Z_N = \frac{1}{p_N} = \sum_{n_0=0}^{N} \prod_{i-n_0+1}^{N} \frac{H_i}{K_{i-1}} \qquad (1.47)$$

is required to obey the normalization condition $\sum_{n_0=0}^{N} p_{n_0} = 1$. The closed form expression for the coefficients H_{n_0} and K_{n_0} can be achieved under different approximations for a different trap shapes. For example, one can apply the so-called "quasithermal" approximation [28], that stems the same relative average occupation number in the excited levels of the trap as in the thermal reservoir:

$$\langle n_k\rangle_{n_0} = \eta_k \sum_{k>0}\langle n_k\rangle_{n0}/\sum_{k'}\eta_{k'} = \frac{(N - \bar{n}_0)}{(\exp(\epsilon_k/T) - 1)\mathcal{H}}. \qquad (1.48)$$

As the result, one obtains the heating and cooling coefficients as following:

$$K_{n_0} = (N - n_0)(1 + \eta), \qquad H_{n_0} = \mathcal{H} + (N - n_0)\eta, \qquad (1.49)$$

where:

$$\mathcal{H} = \sum_{k>0} \eta_k = \sum_{k>0} \frac{1}{\exp(\epsilon_k/T) - 1}, \qquad \eta = \frac{1}{(N - n_0)} \sum_k \langle n_k \rangle_{n_0} \eta_k = \frac{1}{\mathcal{H}} \sum_{k>0} \eta_k^2. \quad (1.50)$$

Thus, the analytical formulas for the distribution function of the condensed bosons and the partition function are:

$$p_{n_0} = \frac{1}{Z_N} \frac{(N - n_0 + \mathcal{H}/\eta - 1)!}{(\mathcal{H}/\eta - 1)!(N - n_0)!} \left(\frac{\eta}{1 + \eta}\right)^{N - n_0}, \quad (1.51)$$

$$Z_N = \sum_{n_0=0}^{N} \binom{N - n_0 + \mathcal{H}/\eta - 1}{N - n_0} \left(\frac{\eta}{1 + \eta}\right)^{N - n_0}. \quad (1.52)$$

The explicit formula (1.51) obeys the same canonical recursion relation, which was discussed previously in Section 3. One should emphasize the specific behavior of the ground state occupation probability distribution function. It evolves from a quasi-thermal peak edged to zero occupation $n_0 = 0$ at $T \approx T_c$ through a narrow peak centered around some $\bar{n}_0 \neq 0$ at $T \approx T_c/2$ to a δ-function-like peak near $n_0 = N$ for a complete Bose-Einstein condensation at $T << T_c$. It is similar to the evolution of the photon number distribution in a laser mode (from thermal to coherent, lasing).

The probability distribution for the total number of non-condensed atoms, $n = N - n_0$,

$$P_n = p_{N-n} = \frac{1}{Z_N} \binom{n + \mathcal{H}/\eta - 1}{n} \left(\frac{\eta}{1 + \eta}\right)^n, \quad (1.53)$$

is complementary to the probability distribution of the number of condensed atoms $n_0 = N - n$. The distribution (1.53) can be named as *a finite negative binomial distribution*, since it has the form of the well known negative binomial distribution

[29]:

$$P_n = \begin{pmatrix} n + M - 1 \\ n \end{pmatrix} q^n (1 - q)^M, \qquad n = 0, 1, 2, ..., \infty, \qquad (1.54)$$

that was so named due to a coincidence of the probabilities P_n with the terms in the negative-power binomial formula:

$$\frac{1}{(1 - q)^M} = \sum_{n=0}^{\infty} \begin{pmatrix} n + M - 1 \\ n \end{pmatrix} q^n. \qquad (1.55)$$

It has similar origin as the well-known binomial distribution,

$$P_n = \begin{pmatrix} M \\ n \end{pmatrix} (1 - q)^n q^{M-n}, \qquad (1.56)$$

which was named after the Newton's binomial formula:

$$[q + (1 - q)]^M = \sum_{n=0}^{M} \begin{pmatrix} M \\ n \end{pmatrix} (1 - q)^n q^{M-n}. \qquad (1.57)$$

The finite negative binomial distribution (1.53) tends to the well-known distribution (1.54) only in the limit $N \gg (1 + \eta)\mathcal{H}$.

The master equation (1.43) for p_{n_0} itself, and the analytic approximate expressions (1.51) and (1.52) for the condensate distribution function p_{n_0} and the partition function Z_N, respectively, are among the main results of the condensate master equation approach. It provides reasonably accurate description of the first two moments of BEC fluctuations in a Bose gas for a large range of parameters and for different trap potentials.

5. Integral representation via the generalized Zeta function

In order to understand relations between various approximate schemes, we formulate a systematic analysis of the equilibrium canonical-ensemble fluctuations of the BEC based on the particle number conserving formalism of Girardeau and Arnowitt [30], the concept of the canonical-ensemble quasiparticles, residue technique and multinomial expansion. This approach will be discussed in details in Chapter II, Section A. In this section I will present an equivalent formulation of the quasiparticle approach in terms of the poles of the generalized Zeta function.

Cumulants (semi-invariants) of the BEC fluctuations in an ideal Bose gas can be written in a equivalent form which is quite interesting mathematically [29]. Namely, starting with the cumulant generating function $\ln \Theta_{ex}(\beta, z)$, where $\beta = 1/k_B T$ and $z = e^{\beta \mu}$,

$$\ln \Theta_{ex}(\beta, z) = -\sum_{\nu=1}^{\infty} \ln(1 - z \exp[-\beta(\epsilon_\nu - \epsilon_0)]) = \sum_{\nu=1}^{\infty} \sum_{n=1}^{\infty} \frac{z^n \exp[-n\beta(\epsilon_\nu - \epsilon_0)]}{n}, \quad (1.58)$$

one can use the Mellin-Barnes transform:

$$e^{-a} = \frac{1}{2\pi i} \int_{\tau - i\infty}^{\tau + i\infty} dt \ a^{-t} \Gamma(t) \quad (1.59)$$

to write:

$$\ln \Theta_{ex}(\beta, z) = \sum_{\nu=1}^{\infty} \sum_{n=1}^{\infty} \frac{z^n}{n} \frac{1}{2\pi i} \int_{\tau - i\infty}^{\tau + i\infty} dt \Gamma(t) \frac{1}{[n\beta(\epsilon_\nu - \epsilon_0)]^t} =$$

$$= \frac{1}{2\pi i} \int_{\tau - i\infty}^{\tau + i\infty} dt \Gamma(t) \sum_{\nu=1}^{\infty} \frac{1}{[\beta(\epsilon_\nu - \epsilon_0)]^t} \sum_{n=1}^{\infty} \frac{z^n}{n^{t+1}}. \quad (1.60)$$

Recalling the series representation of the Bose functions $g_\alpha(z) = \sum_{n=1}^{\infty} z^n/n^\alpha$ and introducing the generalized, "spectral" Zeta function $Z(\beta, t) = [\beta(\epsilon_{nu} - \epsilon_0)]^{-t}$, one

arrives at the convenient (and exact) integral representation:

$$\ln \Theta_{ex}(\beta, z) = \frac{1}{2\pi i} \int_{\tau-i\infty}^{\tau+i\infty} dt \Gamma(t) Z(\beta, t) g_{t+1}(z). \tag{1.61}$$

Applying the well-known relation for the Bose functions $z \frac{d}{dz} g_\alpha(z) = g_{\alpha-1}(z)$ and $g_\alpha(1) = \zeta(\alpha)$, where $\zeta(\alpha)$ denotes the original Riemann Zeta function, Eq. (1.61) can be rewritten in terms of the cumulants of the distribution function as:

$$\kappa_k(\beta) = \left(z \frac{\partial}{\partial z} \right)^k \ln \Theta_{ex}(\beta, z)|_{z=1} = \frac{1}{2\pi i} \int_{\tau-i\infty}^{\tau+i\infty} dt \Gamma(t) Z(\beta, t) \zeta(t + 1 - k). \tag{1.62}$$

Thus, by means of the residue theorem, Eq.(1.62) links all cumulants of the canonical distribution function in the condensate regime to the poles of the generalized Zeta function $Z(\beta, t)$, which contains all the system properties, and to the pole of a system-independent Riemann Zeta function, the location of which depends on the order k of the respective cumulant. The formula (1.62) provides a systematic asymptotic expansion of the cumulants $\kappa_k(\beta)$ through the residues of the analytically continued integrands, taken from right to left. The large system behavior extracted from the condensate fluctuations is definitely seen. The details and examples of such analysis can be found in [20].

I would like to emphasize that none of the presented above theories can describe the mesoscopic behavior of the confined Bose gas in the trap without using some approximations, and there is no yet a complete and general theory of the BEC fluctuations.

C.   Plan of the thesis and brief discussion of the main results

The dissertation is organized as follows in Chapter II, Section A I start with the Girardeau-Arnowitt (GA) [30, 31] particle-number conserving operator formalism of

the canonical ensemble for analyzing the equilibrium fluctuations of the partially condensed Bose gas in a box with the periodic boundary conditions. GA operators can be understood as a creation and annihilation operators of particles in the reduced many-body Fock subspace. New quasiparticles are essentially different from the original and allow one to obey the exact N-particle constraint in a very elegant way, taking into account all possible correlations between bosons. In Chapter II, Section B, I obtain a simple analytical expression for the characteristic function of the ground state occupation number for an ideal gas in the a with the periodic boundary conditions following the approach of [21].

In Chapter II, Section C, I present the calculations of the statistical moments of the ground state occupation number that are valid not only for the low temperature limit up to the close vicinity of the critical temperature, but for the whole temperature range from zero to infinity. This is achieved by introducing the weight to the distribution function of the number of condensed particles. Therefore properly normalized "new" distribution function exactly obeys the well-known recursion relation for an ideal gas and N-particle constraint, by its construction, which makes it truly a solution of the problem. Improved moments and cumulants calculated from this distribution function are in the excellent agreement with the exact numerical results available for an ideal Bose gas via the recursion relation (1.38).

The focus of this work is the central moments $\mu_m = \langle (n - \bar{n})^m \rangle$. For the analysis of non-Gaussian properties it is more convenient to consider cumulants (semi-invariants) κ_m which are related to the central moments μ_m and "generating cumulants" $\tilde{\kappa}_m$ by the following relations:

$$\kappa_1 = \bar{n}, \quad \kappa_2 = \mu_2, \quad \kappa_3 = \mu_3, \quad \kappa_4 = \mu_4 - 3\mu_2{}^2,$$

$$\kappa_5 = \mu_5 - 10\mu_2\mu_3, \quad \kappa_6 = \mu_6 - 15\mu_2\left(\mu_4 - 2\mu_2^2\right), \tag{1.63}$$

$$\kappa_1 = \tilde{\kappa}_1, \quad \kappa_2 = \tilde{\kappa}_2 + \tilde{\kappa}_1,$$

$$\kappa_3 = \tilde{\kappa}_3 + 3\tilde{\kappa}_2 + \tilde{\kappa}_1, \quad \kappa_4 = \tilde{\kappa}_4 + 6\tilde{\kappa}_3 + 7\tilde{\kappa}_2 + \tilde{\kappa}_1, ... \qquad (1.64)$$

In the last two sections of the Chapter II I present the closed-form, analytical expression for the distribution function and obtain its expansion in terms of the multinomial coefficients. Finally, I compare the condensate statistics for the finite system with its thermodynamic limit.

In Chapter III I use another technique to obtain the the ground state occupation statistics. In contrast with Chapter II, where the properly scaled temperature dependences of the distribution function and central moments were studied at a fixed number of particles, I analyze the problem when the temperature is fixed and all the physical quantities are the functions of the number of particles in the trap. In this case the particle number constraint is still working to force BEC, since there is a critical number of particles which is determined by the size of the trap.

This formulation simplifies calculations and gives a better accuracy. It focuses mostly on the vicinity of the critical number of particles, thus corresponds to the vicinity of the critical temperature in the corresponding temperature-dependent expressions. I evaluate numerically the Fourier integral which transforms characteristic function into the distribution function using the Fast Fourier Transformation technique. I present the numerical solution of the problem and obtain the expressions for the first four central moments of the ground state occupation number dependences with respect to the number of particles. Besides that I present the asymptotic solutions for the corresponding distribution function in the region of high and low temperature. In the last section of the Chapter III I analyze the self-similarities of properly scaled BEC fluctuations and extract their actual scale. I also compare these universal expressions with the simple formulas arising from the pure Gaussian distri-

bution function and discuss different possibilities of the universal scale expressions.

In Chapter IV I employ the refined saddle-point approximation to obtain the asymptotic expression for the distribution function of condensed atoms in an ideal gas in a trap. In Section A following [27] I formulate the method for the case of a harmonic trap and explain why the standard saddle point approximation does not work for the systems with condensate. Then in Section B I employ this method to find the condensate distribution function in an ideal gas in a box. In Section C I do numerical simulations and compare the results obtained by the fixed temperature technique in Chapter III and refined saddle-point approximation for the distribution function.

In Appendices A, B, C I present the detailed derivation of the characteristic function and the initial statistical moment of the ground state occupation number. Also I present the residue technique for the condensate fluctuations and derivation of the multinomial expansion approach for the condensate statistics.

In Chapter V I summarize the main results of this work. I discuss the next step in the development of the current theory, namely the transition from ideal gas model to the case of a weakly interacting Bose gas. In particular, I present the expressions for the low and high temperature asymptotics for the first few centered moments of ground state statistics for a weakly interacting Bose gas in the Bogoliubov approximation.

CHAPTER II

QUANTUM STATISTICS OF AN IDEAL BOSE GAS IN A BOX IN THE
CANONICAL ENSEMBLE

A.   Canonical ensemble quasiparticle approach

The standard methods of thermodynamics are not appropriate for the analysis of
BEC fluctuations and mesoscopic effects. For example, the most widely known grand-
canonical approach suffers from the grand-canonical catastrophe [32]. The restricted
ensemble approach, which fixes the amplitude and the phase of the condensate wave
function, is unable to analyze the fluctuation problem at all. To study the fluctua-
tions, one should fix only external macroscopical and global, topological parameters
of the system such as temperature, pressure, number of particles, super-fluid flow
pattern, boundary conditions, etc. Solving the Von Neuman equation with general
initial conditions one can get all possible states of the condensate. For the real sys-
tems, especially with even weaker interactions this way is very complicated. The
perturbative series involving the initially unperturbed grand-canonical ensemble do
not converge [8], thus it is impossible to use them.

One way to handle this problem is to deal with constrained many-body Hilbert
space. The possibility of the proper reduction of the Fock space arises from introduc-
ing the new canonical ensemble quasiparticles. The usual particle number representa-
tion in many-body Hilbert space can be written as a proper combination of creation
and annihilation operators $\hat{a}_{\mathbf{k}}^{\dagger}$ and $\hat{a}_{\mathbf{k}}$, which acts like:

$$\hat{a}_{\mathbf{k}}^{\dagger}|\psi_{\mathbf{k}}^{(n)}\rangle = \sqrt{n+1}|\psi_{\mathbf{k}}^{(n)}\rangle, \quad \hat{a}_{\mathbf{k}}|\psi_{\mathbf{k}}^{(n)}\rangle = \sqrt{n}|\psi_{\mathbf{k}}^{(n-1)}\rangle, \quad \hat{n}_{\mathbf{k}}|\psi_{\mathbf{k}}^{(n)}\rangle = n|\psi_{\mathbf{k}}^{(n)}\rangle. \tag{2.1}$$

Girardeau and Arnowitt (GA) [30, 31] were the first who introduced the creation and

annihilation operators acting in the canonical ensemble subspace of the Fock space which takes into account the particle number constraint. These operators obey the usual Bose commutation relations for $\mathbf{k} \neq 0$ in the subspace with $n_0 \neq 0$, namely,

$$\hat{\beta}^\dagger_{\mathbf{k}} = \hat{a}^\dagger_{\mathbf{k}} \hat{\beta}_0, \quad \hat{\beta}_{\mathbf{k}} = \hat{\beta}^\dagger_0 \hat{a}_{\mathbf{k}}, \quad \hat{\beta}_0 = (1 + \hat{n}_0)^{-1/2} \, \hat{a}_0, \quad \left[\hat{\beta}_{\mathbf{k}}, \hat{\beta}^\dagger_{\mathbf{k}'}\right] = \delta_{\mathbf{k},\mathbf{k}'}. \tag{2.2}$$

Since the GA operator subspace excludes states with zero number of the condensed atoms, this approach will be relevant for almost all temperatures $T < T_c$, starting even from a small condensate fraction $\bar{n}_0 << N$. It especially good for the well peaked ground sate occupation number distribution and relatively small variance in comparison with mean occupation number. Thus, we approximate the exact canonical ensemble H^{CE} subspace by the subspace $H^{\mathrm{CE}}_{n_0 \neq 0}$ with excluded zero condensed fraction states. This means that we are considering the transitions between a condensate state ($\mathbf{k} = 0$) and excited states ($\mathbf{k} \neq 0$). Consequently, one can express all quantum properties of the system using GA operators. For example, the total number of particles is equal to the sum of the number of condensed atoms and excited atoms:

$$\hat{n}_0 = N - \sum_{\mathbf{k} \neq 0} \hat{n}_{\mathbf{k}}, \tag{2.3}$$

where the excited state occupation number is:

$$\hat{n}_{\mathbf{k}} = \hat{a}^\dagger_{\mathbf{k}} \hat{a}_{\mathbf{k}} = \hat{\beta}^\dagger_{\mathbf{k}} \hat{\beta}_{\mathbf{k}}. \tag{2.4}$$

The ground state occupation statistics is very informative part of the BEC fluctuations. Canonical ensemble quasiparticle states can be defined via the bare trap states as their many-body mixture fixed by the interaction and external conditions. Besides that, there are many other quantities which can be defined in a similar way, such as

occupations of the dressed, excited states, etc.

B.   Characteristic function for the ground state occupation number in an ideal Bose gas

From the construction of the canonical-ensemble quasiparticles outlined in the previous section (see Eq. (2.2)), one concludes, that the occupation numbers $n_\mathbf{k}$ can be approximated as an independent stochastic variables and, thus, one can apply an equilibrium distribution to the equilibrium canonical ensemble density matrix:

$$\rho_\mathbf{k}\left(n_\mathbf{k}\right) = \exp\left(-n_\mathbf{k}\epsilon_\mathbf{k}/T\right)\left[1 - \exp\left(-\epsilon_\mathbf{k}/T\right)\right]. \qquad (2.5)$$

The distribution function of the excited atoms according to Eq. (2.3) is just a mirror distribution of the condensed particles:

$$\rho\left(n\right) = \rho_0\left(n_0 = N - n\right). \qquad (2.6)$$

In statistical physics there is a useful formalism of describing the density matrix via the characteristic function.

$$\Theta_n\left(u\right) = \text{Tr}\{e^{iun}\hat{\rho}\}, \qquad \Theta_n\left(u = 0\right) = 1. \qquad (2.7)$$

Taking the inverse Fourier transformation, one obtains the distribution function:

$$\rho\left(n\right) = \frac{1}{2\pi}\int_{-\pi}^{\pi} e^{-inu}\Theta_n(u)\,du. \qquad (2.8)$$

Very important property of the characteristic function is that the characteristic function for the ensemble of the independent stochastic variables is a product of the

individual characteristic functions, thus:

$$\Theta_n\left(u\right) = \prod_{\mathbf{k}\neq 0}\Theta_{n_{\mathbf{k}}}\left(u\right), \qquad \ln\Theta_n\left(u\right) = \sum_{\mathbf{k}\neq 0}\ln\Theta_{n_{\mathbf{k}}}\left(u\right). \tag{2.9}$$

Each individual characteristic function can be easily calculated from the equilibrium density matrix as following:

$$\Theta_{n_{\mathbf{k}}}\left(u\right) = \mathrm{Tr}\{e^{iu\hat{n}_{\mathbf{k}}}\hat{\rho}_{\mathbf{k}}\} = \mathrm{Tr}\{e^{iu\hat{n}_{\mathbf{k}}}e^{-\epsilon_{\mathbf{k}}\hat{n}_{\mathbf{k}}/T}\}\left(1 - e^{-\epsilon_{\mathbf{k}}/T}\right) = \frac{z_{\mathbf{k}} - 1}{z_{\mathbf{k}} - z}, \tag{2.10}$$

where $z_{\mathbf{k}} = \exp\left(\epsilon_{\mathbf{k}}/T\right)$ and $z = \exp(iu)$ is a fugacity. Therefore for an ideal gas in an arbitrary trap, the characteristic function of the number of excited atoms can be written as:

$$\Theta_n\left(u\right) = \prod_{\mathbf{k}\neq 0}\frac{z_{\mathbf{k}} - 1}{z_{\mathbf{k}} - e^{iu}}. \tag{2.11}$$

The characteristic function or its logarithm can be expanded as a Taylor series with cumulants (semi-invariants), generating cumulants or initial (noncentered) moments as the coefficients [29]:

$$\Theta_n(u) = \sum_{m=0}^{\infty}\alpha_m\frac{(iu)^m}{m!}, \qquad \alpha_m \equiv \langle n^m\rangle = \frac{d^m}{d(iu)^m}\Theta_n(u)|_{u=0}, \tag{2.12}$$

$$\ln\Theta_n(u) = \sum_{m=1}^{\infty}\kappa_m\frac{(iu)^m}{m!}, \qquad \kappa_m = \frac{d^m}{d(iu)^m}\ln\Theta_n(u)|_{u=0}, \tag{2.13}$$

$$\ln\Theta_n\left(u\right) = \sum_{\mathbf{k}\neq 0}\ln\left(\frac{z_{\mathbf{k}} - 1}{z_{\mathbf{k}} - z}\right) = \sum_{m=1}^{\infty}\kappa_m\frac{(iu)^m}{m!} = \sum_{m=1}^{\infty}\tilde{\kappa}_m\frac{(e^{iu} - 1)^m}{m!}. \tag{2.14}$$

The cumulants κ_m and generating cumulants $\tilde{\kappa}_m$ can be related by the Stirling numbers of the second kind [29]:

$$\sigma_r^{(m)} = \frac{1}{m!}\sum_{k=0}^{m}(-1)^{m-k}\binom{m}{k}k^r, \qquad (e^x - 1)^k = k!\sum_{n=k}^{\infty}\sigma_n^{(k)}\frac{x^n}{n!}. \tag{2.15}$$

The useful properties is that the cumulant of the sum of independent stochastic

variables is equal to a sum of the partial cumulants $\kappa_r = \sum_{\mathbf{k} \neq 0} \kappa_r^{\mathbf{k}}$. This relation follows from the productivity property of the characteristic function (2.9). Also the cumulants can be simply related to the initial (noncentered) and central moments of the distribution by binomial relations [29]:

$$\mu_r = \sum_{k=0}^{r} (-1)^k \binom{r}{k} \alpha_{r-k} \bar{n}^k, \qquad \alpha_r = \sum_{k=0}^{r} \binom{r}{k} \mu_{r-k} \bar{n}^k \qquad (2.16)$$

$$\bar{n} = \kappa_1, \qquad \left\langle (n - \bar{n})^2 \right\rangle \equiv \mu_2 = \kappa_2, \qquad \left\langle (n - \bar{n})^3 \right\rangle \equiv \mu_3 = \kappa_3,$$

$$\left\langle (n - \bar{n})^4 \right\rangle \equiv \mu_4 = \kappa_4 + 3\kappa_2{}^2,$$

$$\left\langle (n - \bar{n})^5 \right\rangle \equiv \mu_5 = \kappa_5 + 10\kappa_2\kappa_3,$$

$$\left\langle (n - \bar{n})^6 \right\rangle \equiv \mu_6 = \kappa_6 + 15\kappa_2 \left(\kappa_4 + 2\kappa_2^2 \right), \qquad (2.17)$$

$$\kappa_1 = \tilde{\kappa}_1, \qquad \kappa_2 = \tilde{\kappa}_2 + \tilde{\kappa}_1, \qquad \kappa_3 = \tilde{\kappa}_3 + 3\tilde{\kappa}_2 + \tilde{\kappa}_1,$$

$$\kappa_4 = \tilde{\kappa}_4 + 6\tilde{\kappa}_3 + 7\tilde{\kappa}_2 + \tilde{\kappa}_1, ... \qquad (2.18)$$

In the case of low temperatures, far enough from the region near the critical temperature of the Bose condensate, where the properties of the moments except for the average value do not depend on the total number of atoms in a trap, i.e. the mesoscopic effects are not important, the cumulants of the condensate distribution can be written as:

$$\tilde{\kappa}_m = (m-1)! \sum_{\mathbf{k} \neq 0} (e^{\epsilon_{\mathbf{k}}/T} - 1)^{-m}; \qquad \kappa_r = \sum_{n=k}^{\infty} \sigma_n^{(k)} \tilde{\kappa}_m \qquad (2.19)$$

These formulas are valid in the case of condensate inside the infinite reservoir of the excited atoms. This universal result was found in [21] and is valid on the basis of the Maxwell's demon ensemble approximaiton. In particular, this result does not describe most of the mesoscopic effects and the temperature range near and above critical temperature T_c.

C.   Weighted distribution function and cumulants

The approximation of the independent canonical ensemble quasiparticles outlined in the previous section, yields too large values of the fluctuations above the critical temperature of the condensate. It follows from the fact that the presented statistics in general and the distribution function in particular do not depend on the total number of atoms in the trap. Therefore it is true for an infinite number of particles. To improve the previous result, one can construct a "new" distribution function which coincides with the "old" one for low enough temperatures and has a significantly different behavior close and above the critical temperature. This behavior is derived from experimental data and exhibits a smooth decay for all central statistical moments of the ground state occupation number, for instance, see figures on pages 44-46. It can be done by introducing the weighting factor to the distribution function, $\rho(n) \rightarrow \omega(n)\rho(n)$ which will improve the behavior to make it correct. Now, let us analyze the physical structure of the weighted function. The finite constraint implies that the number of particles in the condensate can not be less than zero $(n_0 \geq 0)$, or that the number of excited atoms can not be larger than the total number of particles $(n \leq N)$. One can conclude that the weighted function is somewhat like a theta function, which obeys all the properties listed earlier:

$$\omega(n) = \theta(N - n) \equiv \begin{cases} 1, n \leq N \\ 0, n > N \end{cases} \qquad (2.20)$$

One should properly normalize the distribution function by the factor of

$$\langle \theta(N - n) \rangle = \sum_{n=0}^{\infty} \theta(N - n)\rho(n) = \sum_{n=0}^{N} \rho(n), \qquad (2.21)$$

since the unit normalization is correct only for the infinite sum $\sum_{n=0}^{\infty} \rho(n) = 1$. In other words, we cut the distribution function of the excited states occupation number when it reaches the physical limit, i.e. the total number of particles, and normalize this distribution by the summation over this interval of n. Therefore, the "new" distribution function for the excited states occupation number is:

$$\rho_{new}(n) = \frac{\rho_{old}(n)}{\langle \theta(N-n) \rangle} = \frac{\rho_{old}(n)}{\sum_{n=0}^{N} \rho_{old}(n)}, \tag{2.22}$$

and corresponding initial (noncentered) moments are

$$\alpha_m \equiv \langle n^m \rangle = \frac{\langle n^m \theta(N-n) \rangle}{\langle \theta(N-n) \rangle} = \frac{\sum_{n=0}^{N} n^m \rho_{old}(n)}{\sum_{n=0}^{N} \rho_{old}(n)} = \sum_{n=0}^{N} n^m \rho_{new}(n). \tag{2.23}$$

In the following analysis I will neglect the "new" and "old" subscripts, since all physical quantities are written from now on in terms of the "new" variables.

D. Properties of the spectrum of the box with the periodic boundary conditions

In this section I explain the subtle points of the momentum summation (product) that occurs in the different statistical quantities in an ideal gas in a box with periodic boundary conditions. Consider an atomic gas with a mass M in the large 3D box of a volume L^3 with periodic boundary conditions, which looks almost like a free particle spectrum, beside the certain quantized momentum $\hbar \mathbf{k}_l$

$$\epsilon_{\mathbf{k}} = \frac{\hbar^2 \mathbf{k}^2}{2M}, \qquad \mathbf{k}_l = \frac{2\pi}{L}\mathbf{l}, \qquad \mathbf{l} = (l_x, l_y, l_z). \tag{2.24}$$

The characteristic quantity $z_{\mathbf{k}} = e^{\epsilon_{\mathbf{k}}/T} = e^{\epsilon_1 \mathbf{l}^2/T}$ has the meaning of the inverse probability of finding particle in the state with energy $\epsilon_{\mathbf{k}}$, and the energy gap parameter is:

$$\epsilon_1/T = (2\pi\hbar/L)^2/(2MT). \tag{2.25}$$

It is obvious, that the critical temperature is different for different number of particles, even-though the temperature scale is always the critical temperature for the thermodynamic limit of an ideal gas in a box:

$$T_c = \frac{2\pi\hbar^2}{M} \left(\frac{N}{L^3 \zeta(3/2)} \right)^{2/3}, \tag{2.26}$$

so that:

$$\bar{n}_0 = N - \bar{n} = N - \kappa_1 = N \left[1 - (T/T_c)^{3/2} \right]. \tag{2.27}$$

One can simplify the summation involved in the computation of cumulants and product in characteristic function by applying the symmetry of the boundaries and spectrum. Let us focus on the summation, for instance. One has the sum over all modes beside the mode with zero energy - the excluded zero origin. This summation can be performed over different 3D, 2D, and 1D submanifolds in the momentum space of the box separately. It is obvious that modes with $\mathbf{k}$ and $-\mathbf{k}$ have the same energy. For 3D subspace one has 8 equivalent domains with positive (k_x, k_y, k_z) and 6 ways of rearranging them in the order, for example: $k_x > k_y > k_z$ or $k_x > k_y < k_z$, etc. The total degeneracy will be $8 \cdot 6 = 48$. Similarly, one can obtain the following degeneracies for 2D submanifold: $4 \cdot 3 = 12$ domains for the pair and 2 ways of rearranging $k_x < k_y$ or $k_x > k_y$, thus the total 2D degeneracy is 24. Note, that 1D submanifold contains three types of subvolumes; namely a domain where for example: $k_x \neq 0, k_y = k_z = 0$ with degeneracy $2 \cdot 3 = 6$, corresponding to the ribs of the cube, $k_x = k_y \neq 0, k_z = 0$ with degeneracy $4 \cdot 3 = 12$, corresponding to the diagonals of each of eight sides of the cube and domain with $k_x = k_y = k_z \neq 0$ with degeneracy 8, as a diagonal in each of eight quadrants of positive or negative k-axis. Thus, one can conclude, that the summation (product) of an arbitrary function $f(\mathbf{k})$ over all momentum space with

excluded origin can be written as:

$$\sum_{\mathbf{k}\neq 0} f(\mathbf{k}) = \sum_{\mathbf{k}\equiv(k_x,k_y,k_z)\neq 0} f(k_x,k_y,k_z) = 48 \sum_{k_x\geq k_y>k_z>0} f(k_x,k_y,k_z) +$$

$$24 \sum_{k_x>k_y>0} f(k_x,k_y,0) + 6\sum_{k_x>0} f(k_x,0,0) + 12\sum_{k_x>0} f(k_x,k_x,0)+ \qquad (2.28)$$

$$+8\sum_{k_x>0} f(k_x,k_x,k_x).$$

For example, the characteristic function (2.11) of the total number of noncondensed

particles can be written as:

$$\Theta(z) = \prod_{\mathbf{k}\neq 0} \frac{z_{\mathbf{k}}-1}{z_{\mathbf{k}}-z} = \prod_{k_z=1}^{\infty}\prod_{k_y=k_z+1}^{\infty}\prod_{k_x=k_y}^{\infty} \left(\frac{e^{\epsilon_1(k_x^2+k_y^2+k_z^2)/T}-1}{e^{\epsilon_1(k_x^2+k_y^2+k_z^2)/T}-z} \right)^{48} \times$$

$$\times \prod_{k_y=1}^{\infty}\prod_{k_x=k_y+1}^{\infty} \left(\frac{e^{\epsilon_1(k_x^2+k_y^2)/T}-1}{e^{\epsilon_1(k_x^2+k_y^2)/T}-z} \right)^{24} \prod_{k_x=1}^{\infty} \left(\frac{e^{\epsilon_1(k_x^2)/T}-1}{e^{\epsilon_1(k_x^2)/T}-z} \right)^{6} \times \qquad (2.29)$$

$$\times \prod_{k_x=1}^{\infty} \left(\frac{e^{\epsilon_1(2k_x^2)/T}-1}{e^{\epsilon_1(2k_x^2)/T}-z} \right)^{12} \prod_{k_x=1}^{\infty} \left(\frac{e^{\epsilon_1(3k_x^2)/T}-1}{e^{\epsilon_1(3k_x^2)/T}-z} \right)^{8}.$$

E. Multinomial expansion

The following discussion will be dedicated to the derivation of the closed form ex-

pression for the distribution function, its cumulants, as well as the initial and central

moments using the combinatorial analysis of the multinomial coefficients. The detailed

derivation of the following formalism is presented in Appendices.

Consider the characteristic function of the total number of noncondensed atoms

given in Eqs. (2.9)-(2.11). It can be written as following:

$$\Theta(z) = \prod_{\mathbf{k}\neq 0} \frac{z_{\mathbf{k}}-1}{z_{\mathbf{k}}-z} = \Theta_0 \exp\left(-\sum_{\mathbf{k}\neq 0} \ln(1-z/z_{\mathbf{k}}) \right), \qquad (2.30)$$

where $z = e^{iu}$, $\Theta_0 \equiv \Theta(z=0) = \prod_{\mathbf{k}\neq 0} \frac{z_{\mathbf{k}}-1}{z_{\mathbf{k}}}$ is the characteristic function at zero

fugacity z. Employing the Taylor expansion of the logarithm under the summation

about the point $z = 0$ and changing the summation order in the exponent power, one can rewrite (2.30) as following

$$\Theta(z) = \Theta_0 \exp\left(\sum_{m=1}^{\infty} f_m z^m\right).$$
(2.31)

Employing the approach discussed in the Appendices of expressing the condensate statistics as a residues of the characteristic function evaluated at $z = 0$ (see Eq. (A.4)) one can conclude, that $\rho(n)$ is nothing else but the Taylor coefficient of the z^n term,

$$\rho(n) = \frac{\Theta_0}{n!} \frac{d^n}{dz^n} \left(\sum_{r=0}^{\infty} \frac{1}{r!} \left(\sum_{m=1}^{\infty} f_m z^m\right)^r\right)\Bigg|_{z=0},$$
(2.32)

since all the other are zero. One can now employ the wonderful properties of the multinomial coefficients [29]:

$$\left(\sum_{m=1}^{\infty} f_m z^m\right)^r \equiv r! \sum_{n=r}^{\infty} \frac{z^n}{n!} \sum (n; a_1, a_2, a_3..., a_n)^* f_1^{a_1} f_2^{a_2} f_3^{a_3} ... f_n^{a_n},$$
(2.33)

summed over $a_1 + a_2 + a_3 + ... + a_n = r$ and $a_1 + 2a_2 + 3a_3 + .. + na_n = n$, where the multinomial coefficients have the following closed form expression:

$$(n; a_1, a_2, a_3..., a_n)^* = n!/1^{a_1} a_1! 2^{a_2} a_2! 3^{a_3} a_3! ... n^{a_n} n!,$$
(2.34)

with the same restricted summation $a_1 + 2a_2 + 3a_3 + .. + na_n = n$. The meaning of these coefficients is the number of permutations of $n = a_1 + 2a_2 + 3a_3 + .. + na_n$ symbols composed of a_k cycles of length k for $k = 1, 2, 3, ..., n$.

Applying the expression (2.33) to obtain the distribution function and changing the summation order as well as employing the fact, that n-th derivative is non zero

only for n-th term in the expansion, the result can be written as:

$$\rho(n) = \frac{\Theta_0}{n!} \sum_{m=0}^{n} \sum_{\begin{pmatrix} a_1 + a_2 + ... + a_n = m \\ a_1 + 2a_2 + ... + na_n = n \end{pmatrix}} (n, a_1, a_2, ..., a_n)^* \prod_{j=1}^{n} f_j^{a_j}. \qquad (2.35)$$

This closed form expression for the distribution function is exact and no approxima-
tions were implied so far. The centered analytical moments calculated with such a
distribution function coincide perfectly with the exact recursion relation of Eq. (1.38).

$$\rho_0(n_0) = \frac{Z_{N-n_0}(T) - Z_{N-n_o-1}(T)}{Z_N(T)}; \qquad Z_{-1} \equiv 1, \qquad (2.36)$$

$$Z_N(T) = \frac{1}{N} \sum_{k=1}^{N} Z_1(T/k) Z_{N-k}(T),$$

$$Z_1(T) = 1 + \sum_{\mathbf{k} \neq 0} e^{-\epsilon_{\mathbf{k}}/T}.$$

The perfect match can be confirmed by numerical simulations. The resulting temper-
ature scaled first four central moments of the ground state occupation fluctuations for
an ideal gas in a box, calculated from the Eqs. (2.23) and (2.16) for $N = 100, 500, 1000$
using the multinomial expansion formalism in Eq. (2.35) and exact recursion relation
for an ideal gas in Eq. (2.36) are presented in figures on pages 44-46.

F.   Mesoscopic effects versus the thermodynamic limit

In this section, I summarize the results obtained in the previous section for the meso-
scopic condensate statistics and compare it to the thermodynamic limit statistics,
obtained in [21] for an ideal Bose gas in a box. The first four central moments of
the distribution function in the mesoscopic system can be found by plugging in the
distribution function (2.35) into the expressions for the initial moments (2.23) and for

the central moments (2.16). The expressions for the first four central moments in the thermodynamic limit are obtained through the cumulants (2.19), generating cumulants (2.18), and their connection to the central moments (2.17). For the particular case of an ideal Bose gas in a box it can be written as follows:

$$\tilde{\kappa}_m = (m-1)! \sum_{\mathbf{l}=\{l_x,l_y,l_z\}\neq 0} (e^{\epsilon_1 \mathbf{l}^2/T} - 1)^{-m}; \qquad \kappa_r = \sum_{n=k}^{\infty} \sigma_n^{(k)} \tilde{\kappa}_m, \tag{2.37}$$

where the energy gap parameter ϵ_1 is defined in Eq. (2.25).

$$\bar{n} = \kappa_1, \qquad \left\langle (n-\bar{n})^2 \right\rangle \equiv \mu_2 = \kappa_2, \qquad \left\langle (n-\bar{n})^3 \right\rangle \equiv \mu_3 = \kappa_3,$$

$$\left\langle (n-\bar{n})^4 \right\rangle \equiv \mu_4 = \kappa_4 + 3{\kappa_2}^2. \tag{2.38}$$

If the temperature is much smaller than the energy gap $T << \epsilon_1$, all cumulants and moments become the same, starting with the variance

$$\mu_m \approx \kappa_m \approx \kappa_1 \approx f_1 \propto \left(\frac{T}{T_c}\right)^{3/2} N, \qquad m \geq 2, \tag{2.39}$$

since all $f_m << f_1$ are exponentially small for $m \geq 2$ as follows:

$$\tilde{\kappa}_m \approx f_m \approx 6(m-1)! e^{-m\epsilon_1/T}. \tag{2.40}$$

Thus, the low temperature distribution of the number of noncondensed atoms is Poissonian, and therefore, the condensed atoms are distributed as a "mirror" image (non-Poissonian) as $n_0 = N - n$. This result agrees with the previous calculations [21] for the low temperature behavior in the thermodynamic limit. It can be simply performed, expanding formula (2.35) at low temperature. This consistency is not surprising, since in the low temperature region, the finite number of particles does not play an important role in the evaluation. High temperature asymptotics differ much from the previous calculations. It can be seen from the expressions in Eq. (2.19) for

the cumulants, that all the moments are anomalously large and lowest-energy-mode dominates, i.e., formally infrared divergent. One can expand $\exp(\epsilon_1 \mathbf{l}^2/T) - 1 \approx \epsilon_1 \mathbf{l}^2/T$, so that

$$\kappa_m \approx \tilde{\kappa}_m \propto T^m \propto N^{2m/3}, \qquad m \geq 2. \tag{2.41}$$

In this case even the variance should be calculated from the Eq. (2.19) as a discrete sum:

$$\mu_2 = \kappa_2 N^{4/3} \left(\frac{T}{T_c}\right)^2 \frac{s_4}{\pi^2 [\zeta(3/2)]^{4/3}}, \tag{2.42}$$

where ζ is the zeta function of Riemann,

$$s_4 = \sum_{\mathbf{l} \neq \mathbf{0}} \frac{1}{\mathbf{l}^4}, \tag{2.43}$$

and T_c is the standard critical temperature in the thermodynamic limit, which was defined in Eq. (2.26). It is worth noting that an excess coefficient, i.e. the fourth cumulant normalized by the variance to the fourth power,

$$\gamma_2 \equiv \frac{\kappa_4}{\kappa_2^2} \to const \neq 0, \tag{2.44}$$

remains finite in the thermodynamic limit $N \to \infty$. Therefore, it is clear that the condensate fluctuations are not Gaussian in the thermodynamic limit.

The multinomial approach corrects the temperature dependence of the cumulants. The resulting expression exhibits a decay at high temperatures that is consistent with the grand canonical result for an ideal gas, a result, which is physically reasonable, since at high temperature the condensate fraction is almost zero and the gas behaves like classical ideal gas:

$$\kappa_m \approx \tilde{\kappa}_m \propto (T/T_c)^{-3/2}. \tag{2.45}$$

The grand-canonical approach gives, for instance, the mean ground state occupation

number $\bar{n}_0$ satisfying the self-consistent equation:

$$N - \bar{n}_0 = \sum_{\mathbf{k} \neq 0} \frac{1}{\left(1 + \frac{1}{\bar{n}_0}\right) e^{\epsilon_{\mathbf{k}}/T} - 1}. \tag{2.46}$$

In the case when $T \gg T_c$ the condensate fraction is small $\bar{n}_0 \ll 1$, and therefore one can expand the right hand side of Eq. (2.46). Combining the terms with $\bar{n}_0$, one can obtain the following result:

$$\bar{n}_0 \approx \frac{N}{1 + \sum_{\mathbf{k} \neq 0} e^{\epsilon_{\mathbf{k}}/T}}. \tag{2.47}$$

The summation in the denominator can be performed in the continuum limit, neglecting the excluded point of zero energy, since we are considering an ideal gas model, that yields:

$$\bar{n}_0 \approx \zeta\left(\frac{3}{2}\right)\left(\frac{T}{T_c}\right)^{-3/2}, \tag{2.48}$$

which confirms the analytical asymptotics of the formula (2.45) at high enough temperatures. The comparison between the multinomial expansion approach and the thermodynamic limit for the first four central moments is presented in Figs. 2-6.

Concluding the whole chapter, I briefly emphasize its main points. First, I constructed the set of new canonical ensemble quasiparticles (GA operators) which take into account the particle number constraint. Using the outlined method I analyzed the structure of the characteristic function of the total number of noncondensed atoms. Then I introduced the new properly normalized distribution function, which correctly describes the behavior of the ground-state fluctuations in any temperature regime, which was constructed from the simple physical reasons. I considered the asymptotic expressions for the fluctuations and compared them with the well know grand canonical formalism for high temperatures. I obtained the numerical dependences for the fluctuations for the mesoscopic system of an ideal gas in a box with periodic bound-
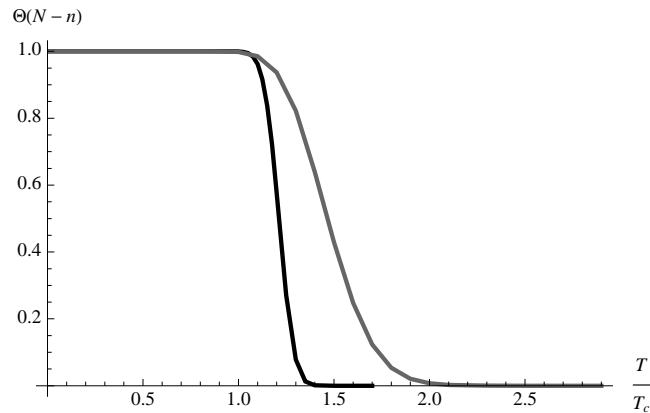
Fig. 2. Temperature scaling of the normalization factor, i.e. $\Theta(N-n)$ for an ideal Bose gas ($N = 100$ - grey line, $N = 1000$ - black line). Temperature is normalized by the standard thermodynamic limit critical value $T_c(N = \infty)$ that differs from the finite-size $T_c(N)$ as is clearly seen in graphs.
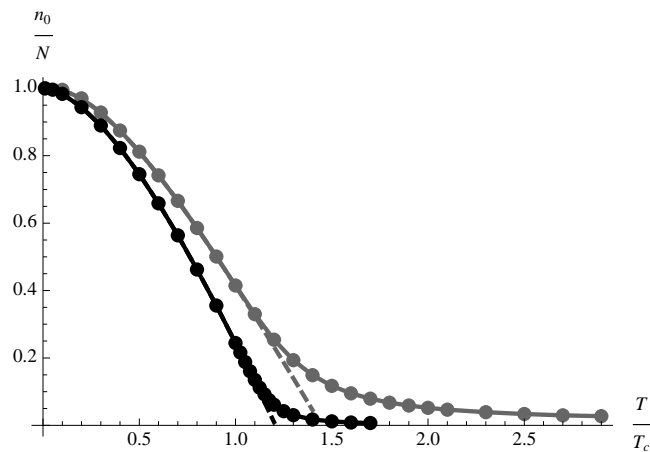
Fig. 3. Temperature scaling of the mean value of the ground state occupation fluctuations for an ideal Bose gas ($N = 100$ - grey, $N = 1000$ - black) obtained from thermodynamic limit expression in Eq. (2.19) - (dashed lines) compared with the multinomial expansion in Eq. (2.35) - (dotted lines) and with the exact recursion relation for an ideal gas in Eq. (2.36) - (solid lines). The multinomial expansion result is almost indistinguishable from the recursion relation as it is clearly seen in graphs.
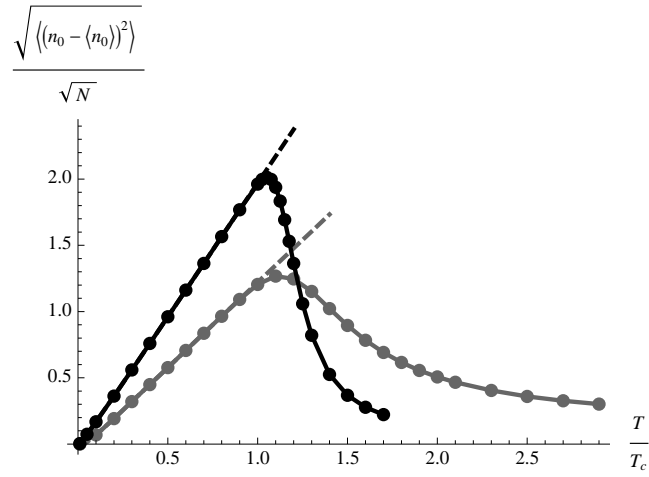
Fig. 4. Temperature scaling of the variance of the ground state occupation fluctuations for an ideal Bose gas ($N = 100$ - grey, $N = 1000$ - black) according to Eq. (2.19) - (dashed lines), Eq. (2.35) - (dotted lines), and Eq. (2.36) - (solid lines).
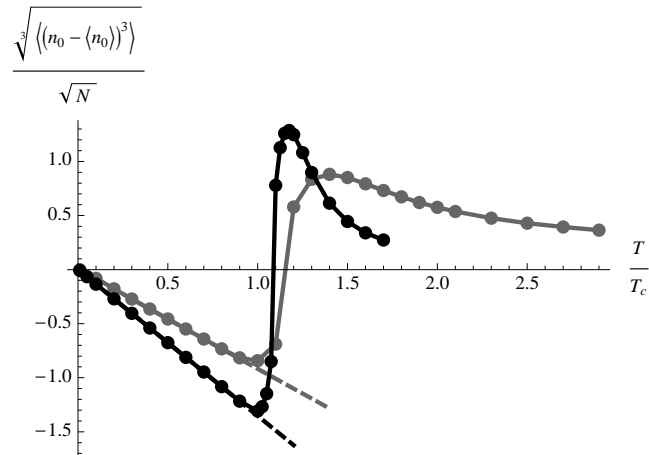
Fig. 5. Temperature scaling of the third central moment μ_3 of the ground state occupation fluctuations for an ideal Bose gas ($N = 100$ -grey, $N = 1000$ - black) according to Eq. (2.19) - (dashed lines), Eq. (2.35) - (dotted lines), and Eq. (2.36) - (solid lines).
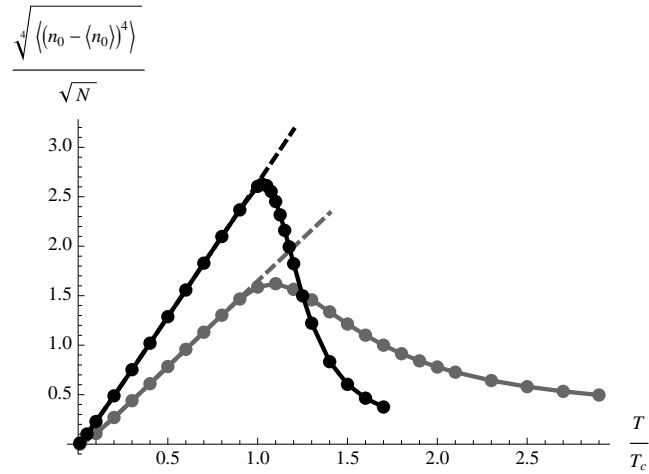
Fig. 6. Temperature scaling of the fourth central moment μ_4 of the ground state occupation fluctuations for an ideal Bose gas ($N = 100$ - grey, $N = 1000$ - black) according to Eq. (2.19) - (dashed lines), Eq. (2.35) - (dotted lines), and Eq. (2.36) - (solid lines).

ary conditions as well. All the listed calculations are valid for the whole temperature range from zero to infinity.

In the next chapter I will discuss another approach in analyzing these fluctuations, in the vicinity of the critical temperature.

CHAPTER III

FIXED TEMPERATURE ANALYSIS OF THE BEC FLUCTUATIONS

A.   Fixed temperature technique

The essence of this chapter is the development of a formalism which allows for a more efficient calculation and a detailed analysis of the BEC fluctuations in the vicinity of the critical temperature. In the previous chapters I presented a technique based on the fixed total number of particle and I analyzed the temperature dependence of the fluctuations. Another approach is to assume that the temperature is fixed and let the number of particles vary. In this sense the temperature and the number of particles are analogue of a conjugate variables. As it was known before, for an arbitrary trap one introduces the critical temperature T_c in the thermodynamic limit, above which there is no condensate in the system. This temperature depends only on the size of the trap and the total number of particle in the system. Assume now that the temperature in the system is constant and equal to the critical temperature, but the number of particles can be changed, then the maximum number of particles in the system is "critical", i.e. number of particles corresponding to the critical temperature. Therefore, one can analyze the structure of the statistical moments of the ground state occupation number with respect to the total number of particles in the system which now can vary but still is constrained by the size of the trap, and thus is a known constant.

The relation between a given temperature T and the critical number of particles for a given trap size is given by the following equation:

$$T = \frac{2\pi\hbar^2}{M} \left(\frac{N_c}{L^3 \zeta(3/2)} \right)^{2/3},$$

(3.1)
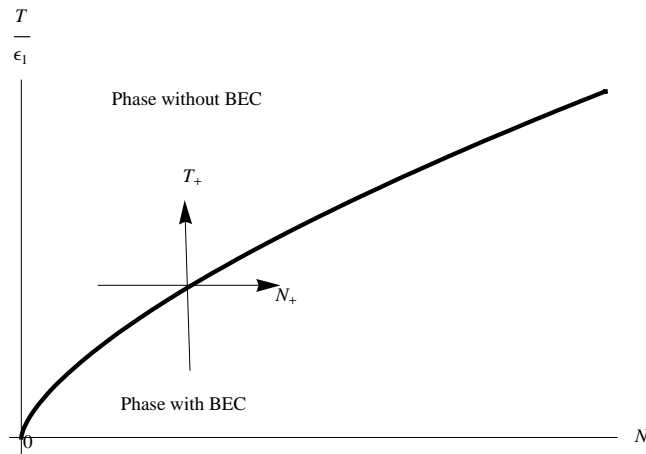
Fig. 7. BEC phase transition diagram for study of the mesoscopic effects. The temperature axis is scaled to the energy gap ϵ_1 in accord with Eq. (2.25).

that determines a formal border between the states with and without BEC in the phase diagram on the plane of the parameters T and N as is shown in Fig. 7. The fixed temperature technique is formed on the studies of the mesoscopic effects when N crosses the initial value N_c and T =const along the direction N_+ as it is shown in Fig. 7. Meanwhile in a standard treatment of the second-order phase transitions people usually study the effects when T crosses the critical temperature T_c and N =const along the direction T_+ (see Fig. 7).

One can now invert (3.1) in a way that the critical number of particles is defined in terms of the fixed temperature. Any quantity is a function of the number of atoms in the trap. For example the cumulants $\kappa_m(N,T) = \kappa_m(N,N_c)$ are functions of N, N_c, and T =const.

It turns out that this approach is more powerful in the sense of a numerical analysis. It allows one to study in details the systems with the large total number of particles, $N \approx 10^4 - 10^7$. It is large enough to ensure that properties of such a systems will be very close to those in the thermodynamic limit. Of course it is just

an approximation, but quantitatively it works with a great accuracy. I will employ the Fast Fourier Transformation technique to evaluate the integral in Eq. (2.8) and furthermore, I will plot the fluctuation statistics dependences with respect to the upper limit of the sum in Eqs. (2.22), (2.23), i.e. the total number of particles in the trap.

B.   Fast Fourier Transformation numerical analysis

I start with evaluating the Fourier integral in Eq. (2.8) by employing the FFT (Fast Fourier Transformation)[29] - the discrete approximation for the integral. The distribution function is localized in the vicinity of $N = N_c$ and decays very fast at smaller values of the argument. In fact, it is almost zero in the region with $N < s \equiv N_c - \alpha\sqrt{\kappa_2}$, where α is a constant of the order of 5. The value of α slightly varies depending on the size of the trap. I will assume the distribution function to be zero in that region. I checked numerically that the approximation does not change the numerical error, which remains to be totally due to rounding to a finite number of the significant figures in computer simulations, and does not exceed a certain value of the order of 10^{-20}. This approximation allows us to shift the domain of the integration to the region of sufficiently non zero values of the $\rho(N)$.

Thus, the distribution function can be written as follows:

$$\rho(n) = \frac{1}{2\pi} \int_{-\pi}^{\pi} e^{-inu} \Theta_n(u)\, du \equiv \frac{1}{m} \sum_{r=1}^{m} \left(e^{-2\pi i s r/m} \Theta_n\left(\frac{r}{m}\right) e^{-2\pi i (r-1)(n-1)/m} \right), \quad (3.2)$$

where m is the dimension of the array and $u = r/m$ is a discrete argument of the characteristic function. The result of evaluation (3.2) is presented in figure on page 59. The crucial advantage of this method is that one needs to evaluate the Fourier transformation only once, for a single value of the temperature and then compute the

analytical moments as functions of the upper limit of the sum. This approach yields to faster results than the evaluation of the Fourier integral for different temperature points when the number of particles is as large as of the order of 10^5 and higher.

The macroscopic order parameter $\langle \Psi_0(N) \rangle = \langle \sqrt{n_0(N)} \rangle$ in Eq. (3.3), the ground state occupation number in Eq. (3.4) $\langle n_0(N) \rangle$ and its fraction in the total system $\langle n_0(N)/N \rangle$ are calculated and plotted as the functions of the number of particles in Figs. 8, 9, and 10 respectively. Three curves correspond to $N = 100$ - (dashed line), $N = 1000$ - (gray line) and $N = 10000$ - (solid black line) number of atoms in a box. The dotted curve is calculated in accord with Landau theory of phase transition in the mean field approximation $\sqrt{n_0} \propto (T - T_c)^{1/2} \propto (N - N_c)^{1/2}$, and therefore $n_0 \propto N - N_c$. It can be seen that for large number of particle starting with $N = 1000$ the shape of the curve follows the mean field approximation, which was obtained in the thermodynamic limit. For $N = 100$ the curve at large N becomes close to the thermodynamic limit, which corresponds to low temperature region, as expected. The mesoscopic region at low N is broad for small number of atoms,

$$\langle \sqrt{n_0(N)} \rangle = \sum_{n=0}^{N} (N - n)^{1/2} \rho(n), \tag{3.3}$$

$$\langle \frac{n_0(N)}{N} \rangle = \frac{1}{N} \langle n_0(N) \rangle = \frac{1}{N} \sum_{n=0}^{N} (N - n) \rho(n), \tag{3.4}$$

The variance of the macroscopic order parameter $\langle \left(\sqrt{n_0(N)} - \overline{\sqrt{n_0(N)}} \right)^2 \rangle$ in Eq. (3.5) is plotted as a function of the number of particles in Fig. 11 for the $N = 100$ - (dashed line), $N = 1000$ - (gray line) and $N = 10000$ - (solid black line) atoms in a box. The variance of the ground state occupation number in Eq. (3.6) is plotted in Fig. 12 for $N = 100$ and in Fig. 13 for $N = 1000$ atoms in a trap. One can see, that in the region of small values of argument for small enough total number of
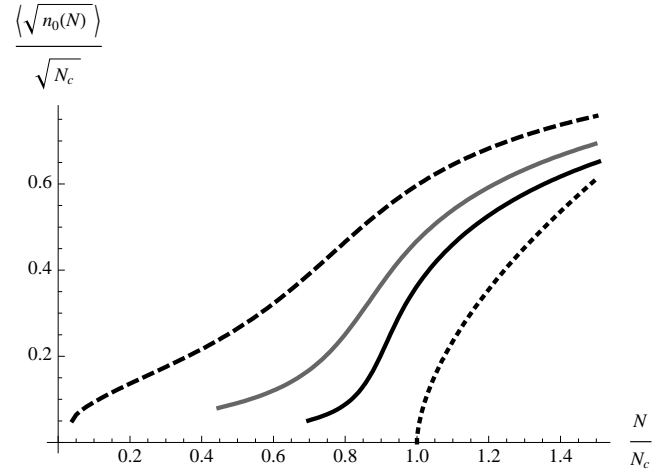
Fig. 8. Macroscopic order parameter (condensate wave function) for $N = 100$ - (dashed line), $N = 1000$ - (grey line), and $N = 10000$ - (solid black line) atoms in a box calculated via the FFT technique in accord with Eq. (3.3) compared with the mean field approximation $\sqrt{n_0} \propto (T - T_c)^{1/2} \propto (N - N_c)^{1/2}$ in the thermodynamic limit - (dotted black line).

Fig. 9. Mean number of condensed atoms for $N = 100$ - (dashed black line), $N = 1000$ - (solid grey line), and $N = 10000$ - (solid black line) atoms in a box calculated via the FFT technique in accord with Eq. (3.4) compared with the mean field approximation $n_0 \propto N - N_c$ in the thermodynamic limit - (dotted black line).

$$\left\langle \frac{n_0(N)}{N} \right\rangle$$

Fig. 10. Mean fraction of condensed atoms for $N = 100$ - (dashed black line), $N = 1000$ - (solid grey line), and $N = 10000$ - (solid black line) atoms in a box calculated via the FFT technique in accord with $\langle n_0(N)/N \rangle$ compared with the mean field approximation $n_0/N \propto 1 - N_c/N$ in the thermodynamic limit - (dotted black line).

atoms in a trap ($N = 100$) the variance of the order parameter does not go to zero, in contrast with the case of large total number of atoms. Also, for large argument all curves go to zero, corresponding to the low temperature exponential decay (see Eq. (2.40)). The variance of ground state occupation number goes to zero at low N for both cases of $N = 100, 1000$. The difference is that the behavior at $N = 1000$ is more sharp compare to broad curve at $N = 100$,

$$\left\langle \left(\sqrt{n_0(N)} - \overline{\sqrt{n_0(N)}} \right)^2 \right\rangle = \langle n_0(N) \rangle - \langle \sqrt{n_0(N)} \rangle^2 =$$

$$= \sum_{n=0}^{N} (N - n)\rho(n) - \left(\sum_{n=0}^{N} \sqrt{N-n}\rho(n) \right)^2, \tag{3.5}$$

$$\mu_2(N) = \langle (n_0(N) - \overline{n_0(N)})^2 \rangle = \langle n_0^2(N) \rangle - \langle n_0(N) \rangle^2 = \langle n^2(N) \rangle - \langle n(N) \rangle^2 =$$

$$= \sum_{n=0}^{N} n^2 \rho(n) - \left(\sum_{n=0}^{N} n\rho(n) \right)^2. \tag{3.6}$$

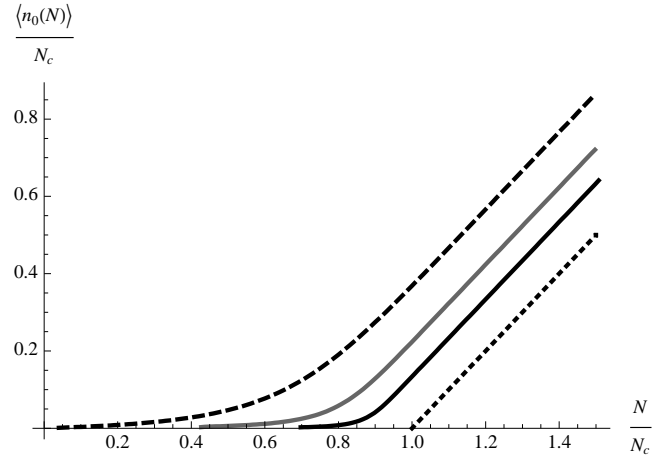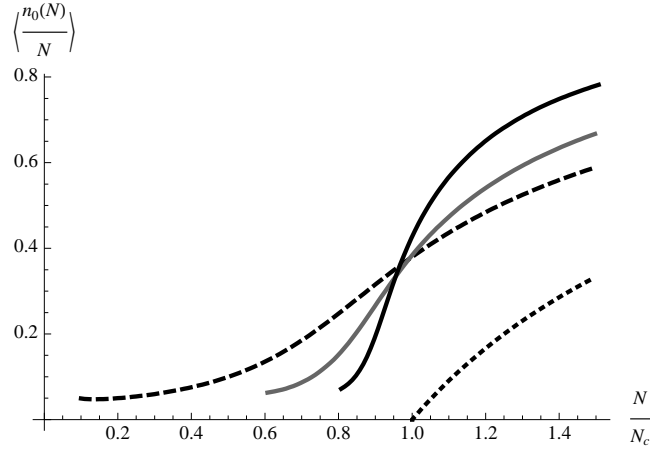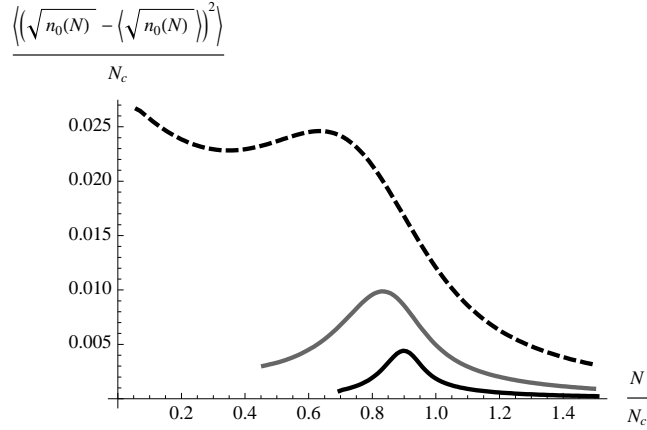Fig. 11. Variance of macroscopic order parameter for $N = 100$ - (dashed black line), $N = 1000$ - (solid grey line), and $N = 10000$ - (solid black line) atoms in a box calculated via the FFT technique in accord with Eq. (3.5).

The central third moment in Eqs. (3.7) is plotted with respect to number of particles for $N = 100$ (Fig. 14) and $N = 1000$ (Fig. 15) total number of atoms in a box. The third central moment and the third cumulant are characterizing the asymmetry of the distribution function from the purely symmetric Gaussian function. Thus, they can be both negative and positive for the different values of argument. The curve for $N = 100$ is more smooth and broad compared to the case of $N = 1000$, which makes the corresponding distribution function more sharp and asymmetric for the case of $N = 1000$ compared to the case of $N = 100$:

$$\mu_3(N) = \langle (n_0(N) - \overline{n_0(N)})^3 \rangle = -\langle (n(N) - \overline{n(N)})^3 \rangle =$$

$$= -\langle n^3(N) \rangle + 3\langle n^2(N) \rangle \langle n(N) \rangle - 2\langle n(N) \rangle^2. \tag{3.7}$$

The central fourth moment in Eq. (3.8) is plotted with respect to the number of
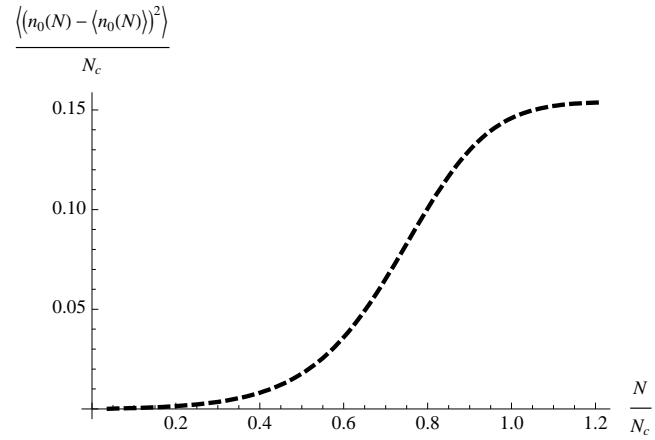
Fig. 12. Variance of condensed atoms for $N = 100$ atoms in a box calculated via the FFT technique in accord with Eq. (3.6).
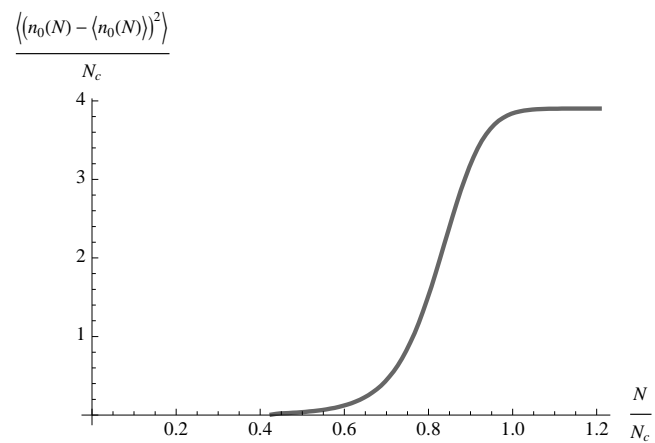
Fig. 13. Variance of condensed atoms for $N = 1000$ atoms in a box calculated via the FFT technique in accord with Eq. (3.6).

$$\frac{\left\langle \left(n_0(N) - \left\langle n_0(N) \right\rangle \right)^3 \right\rangle}{N_c^{3/2}}$$
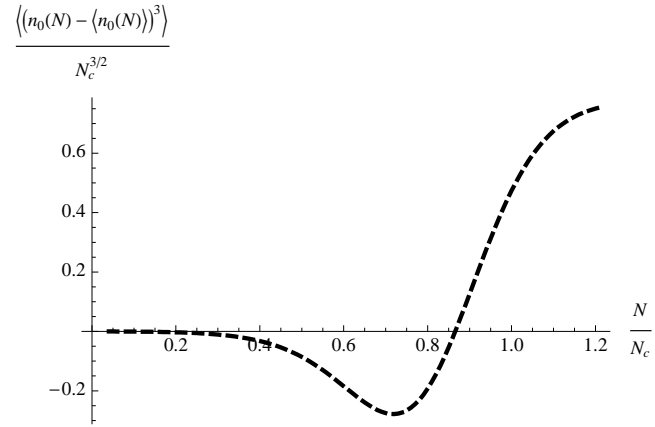
Fig. 14. Third central moment of condensed atoms for $N = 100$ atoms in a box calculated via the FFT technique in accord with Eq. (3.7).

$$\frac{\left\langle \left(n_0(N) - \left\langle n_0(N) \right\rangle \right)^3 \right\rangle}{N_c^{3/2}}$$
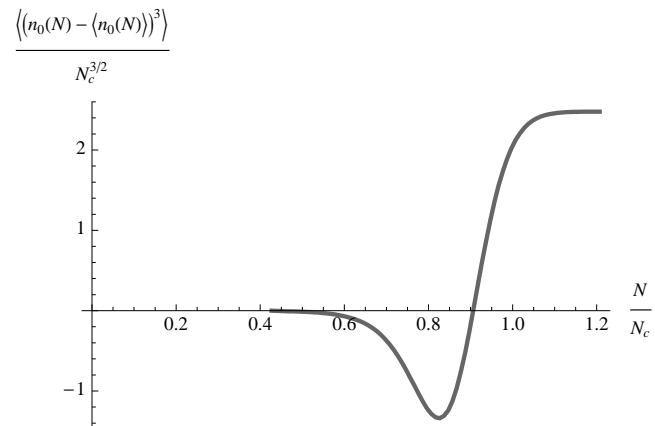
Fig. 15. Third central moment of condensed atoms for $N = 1000$ atoms in a box calculated via the FFT technique in accord with Eq. (3.7).

$$\frac{\left\langle \left(n_0(N) - \langle n_0(N) \rangle\right)^4 \right\rangle}{N_c^2}$$
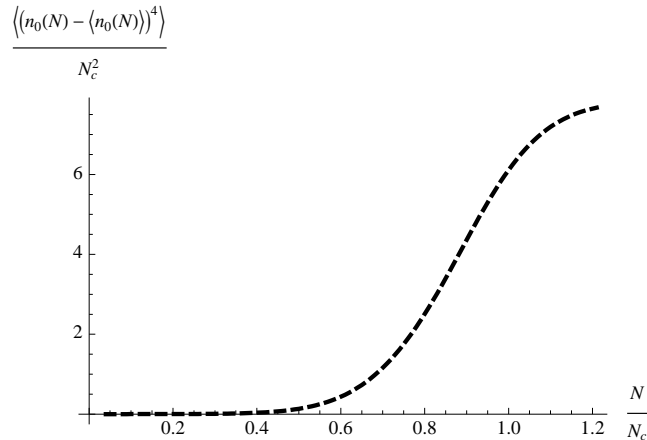
Fig. 16. Fourth central moment of condensed atoms for $N = 100$ atoms in a box calculated via the FFT technique in accord with Eq. (3.8).

particles for $N = 100$ (Fig. 16) and $N = 1000$ (Fig. 17) total number of atoms in the trap. The fourth central moment and the fourth cumulant are very important characteristics of non-Gaussian distributions, related to the excess coefficient (in particular hydrodynamic processes the "flatness" coefficient). The shape of these curves should be similar to the variance, but have sharper character and a more rapid tendency to zero. The curve for $N = 100$ is more smooth and broad compared to the case of $N = 1000$,

$$\mu_4(N) = \langle (n_0(N) - \overline{n_0(N)})^4 \rangle = \langle (n(N) - \overline{n(N)})^4 \rangle =$$

$$= \langle n^4(N) \rangle - 4 \langle n^3(N) \rangle \langle n(N) \rangle^2 + 6 \langle n^2(N) \rangle \langle n(N) \rangle^2 - 3 \langle n(N) \rangle^4. \tag{3.8}$$

The shapes of the curves are similar to the corresponding previous results represented in Figs. 3 - 6. The two methods, discussed in the current chapter and in Chapter II provide in a sense the mirror dependences, namely, the low temperature in the first method corresponds to the large number of particles in the second method and vice versa. This is especially accurate in the vicinity of the critical point. The

$$\frac{\left\langle \left(n_0(N) - \langle n_0(N) \rangle \right)^4 \right\rangle}{N_c^2}$$
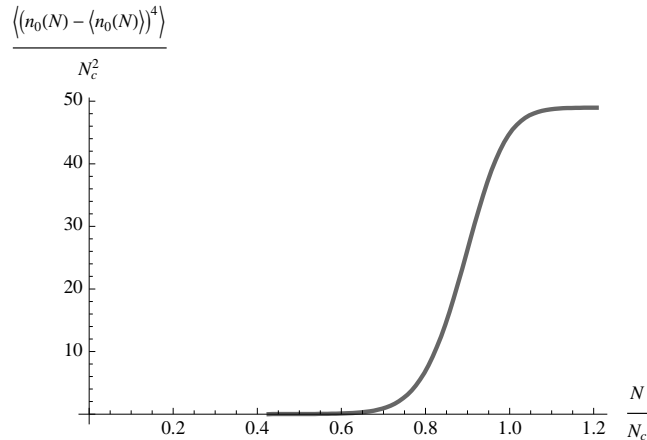
Fig. 17. Fourth central moment of condensed atoms for $N = 1000$ atoms in a box calculated via the FFT technique in accord with Eq. (3.8).

problem with the current approach is that in order to evaluate the distribution function and its moments at very low temperatures, one needs to calculate the Fourier integral in Eq. (3.2) for a very large array of numbers, which is not possible for a typical physical systems. Thus, I will be focused in providing a numerical analysis of the mesoscopic effects in the most interesting critical region.

C.   Self-similarity in BEC fluctuations

In this section, I analyze the structure of BEC fluctuations in the sense of their similarities. The idea is the following: analyzing the natural scales of the fluctuations, one can guess the simple analytical expression for them, which then can be checked asymptotically with the exact solutions (see Chapter IV). In this case, one can compare the properly scaled fluctuations and state, that if the dimensionless functions (functions with no free parameters) as the graphical illustrations will match for different trap size or total particle number, then these scales were guessed correctly, or vice versa. Obviously, such a universality is expected in the thermodynamic limit.

Let us discuss the natural scale of the distribution function of condensed atoms for an ideal gas in a box. First of all, the distribution function should be characterized by some height and width. The width scale is related to the variance and to the approximation of the distribution function by the Gaussian function. One can plot the distribution function for different number of particles scaled to its particular variance and normalized by the maximum value $\rho(\bar{n})$ that is close to the value of the distribution function at the mean occupation number of the excited states $\bar{n} = N - \bar{n}_0$. As it is seen in Fig. 18, a difference between the normalized distribution functions is present only in the regions far away from the maximum, and is of the order of several percents for the sufficient range of the argument. Part of this difference is due to rounding in numerical simulation and can be decreased by increasing the precision of the FFT calculation, since the regions of large deviation arise when the particular value of the distribution function is of the order of 10^{-15} or less (Fig. 19). Hence, the finite number of terms in calculation of the mean occupation number as well as variance can strongly affect the result.

It would be also interesting to find a universal behavior of the wings of the distribution function, considering the width of the function as a fixed value and the value at the maximum point as a free parameter. However, it will be discussed elsewhere.

One can also try to extract the universal scale for the ground state occupation moments, namely for the mean ground state occupation number. In Fig. 20 I present the numerical result, which describes the total number of particles N as function of mean ground state occupation number $\bar{n}_0$. I assume the universal scale of this function to be the same as in the case of distribution function, namely the thermal dispersion Δ, which is defined in Eq. (3.11). The result of the fitting the curves for different number of particles, namely $N = 100,\ 1000?$ by the universal function
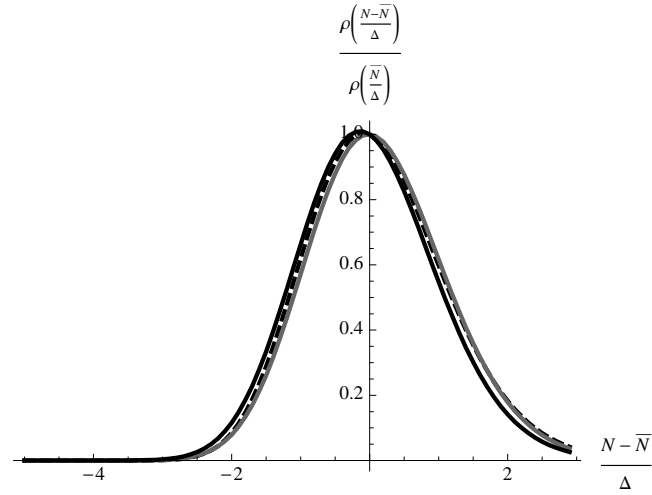
Fig. 18. Scaled noncondensate distribution function for $N = 100$ - (dashed black line), $N = 1000$ - (solid grey line), and $N = 10000$ - (solid black line) atoms in a box calculated via the FFT technique in accord with Eq. (3.2).
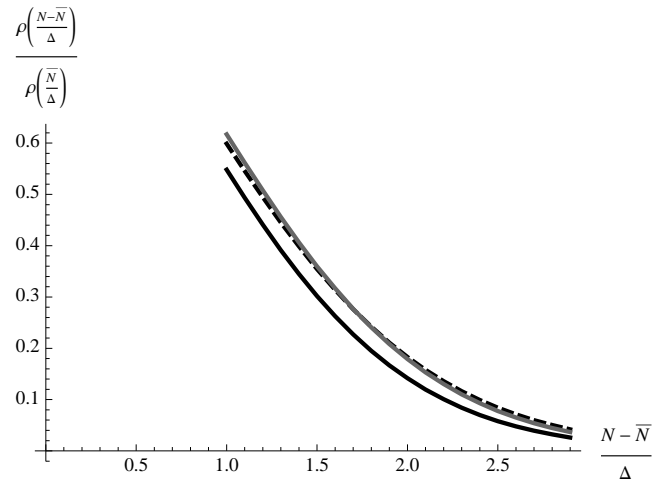
Fig. 19. Scaled noncondensate distribution function for $N = 100$ - (dashed black line), $N = 1000$ - (solid grey line), and $N = 10000$ - (solid black line) atoms in a box calculated via the FFT technique in accord with Eq. (3.2) for large values of argument $N >> \bar{N}$.
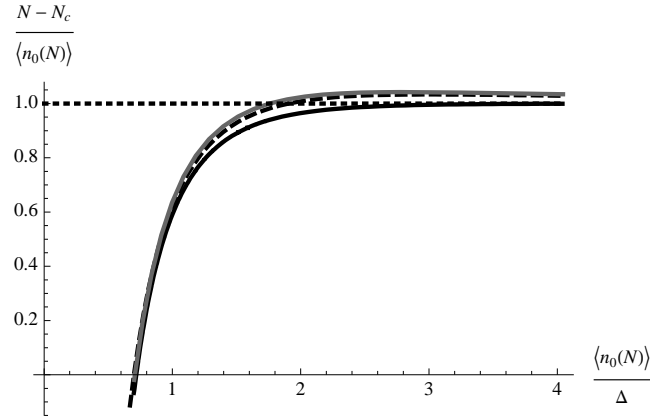
Fig. 20. The ratio of the total number of particles in a box N shifted by the critical number N_c and the mean ground state occupation number $\bar{n}_0$ as a function of the properly scaled argument $\bar{n}_0/\Delta$ for $N = 100$ - (dashed black line) and $N = 1000$ - (solid grey line) atoms in a box calculated via the FFT technique, the numerical fit in accord with Eq. (3.9) - (solid black line), and the mean field approximation $N - N_c = \bar{n}_0$ - (dotted black line).

yields the following expression:

$$\frac{N - N_c}{\bar{n}_0} = 1 - \frac{\exp\left(-2\frac{\bar{n}_0}{\sqrt{2}\Delta}\right)}{\left(\frac{\bar{n}_0}{\sqrt{2}\Delta}\right)^{3/2}} \tag{3.9}$$

and is plotted in Fig. 20. One can see the good agreement between graphs and the expected tendency to the thermodynamic limit result, calculated via the mean field approximation. This result confirms the initial guess of the characteristic scale of the BEC fluctuations to be the thermal dispersion Δ. The approach which led to this result will be developed somewhere else.

One can analyze the structure of the fluctuations if the distribution function would be a pure Gaussian function.The Gaussian anzats can be used as an estimate, and are very useful for consistency of the present discussion. So let the distribution

function be described by:

$$\rho(n) \approx \frac{1}{\sqrt{2\pi}\Delta} \exp\left(-\frac{(n-\bar{n})^2}{2\Delta^2}\right), \tag{3.10}$$

with characteristic parameters of the mean value and dispersion defined as

$$\bar{n} = \sum_{\mathbf{k}\neq 0} \frac{1}{\exp(\epsilon_{\mathbf{k}}/T) - 1} \qquad \text{and} \qquad \Delta = \langle (n-\bar{n})^2 \rangle. \tag{3.11}$$

One can check that close to the maximum value, the distribution function is almost Gaussian (see Figs. 21 and 22), but far away, where the contributions from the wings are more important, the distribution function is essentially non-Gaussian. These features are clearly seen in Fig. 18 plotted for the total number of particles $N = 10000$. Let us calculate the initial moments of this Gaussian distribution function as:

$$\bar{n}^k(N) = \sum_{n=0}^{N} n^k \rho(n) \approx \frac{\int_0^N x^k \frac{1}{\sqrt{2\pi}\Delta} \exp\left(-\frac{(x-\bar{n})^2}{2\Delta^2}\right) dx}{\int_0^N \frac{1}{\sqrt{2\pi}\Delta} \exp\left(-\frac{(x-\bar{n})^2}{2\Delta^2}\right) dx}, \tag{3.12}$$

where I used the continuum limit. The result for the mean occupation number of the ground state is:

$$\bar{n}_0(N) \approx$$

$$\approx \frac{e^{-\frac{N^2+\bar{n}^2}{2\Delta^2}}\left(2\left(-e^{\frac{N^2}{2\Delta^2}} + e^{\frac{N\bar{n}}{\Delta^2}}\right)\Delta + e^{\frac{N^2+\bar{n}^2}{2\Delta^2}}\sqrt{2\pi}\left(\mathrm{erf}\left(\frac{\bar{n}-N}{\sqrt{2}\Delta}\right) - \mathrm{erf}\left(\frac{\bar{n}}{\sqrt{2}\Delta}\right)\right)(\bar{n}-N)\right)}{\sqrt{2\pi}\left(\mathrm{erf}\left(\frac{\bar{n}}{\sqrt{2}\Delta}\right) - \mathrm{erf}\left(\frac{\bar{n}-N}{\sqrt{2}\Delta}\right)\right)}, \tag{3.13}$$

where $\mathrm{erf}(x) = 2/\sqrt{\pi}\int_0^x e^{-t^2} dt$ is a standard error function. Higher order moments can also be written in the similar way, but I will not discuss them here.

The mean occupation number calculated by the FFT technique versus Gaussian approximation is presented in Figs. 23 and 24. One can see that close to the mean occupation number, the graphs are almost indistinguishable, even for relatively small total number of particles $N = 1000$, but far away the deviation is increasing. It
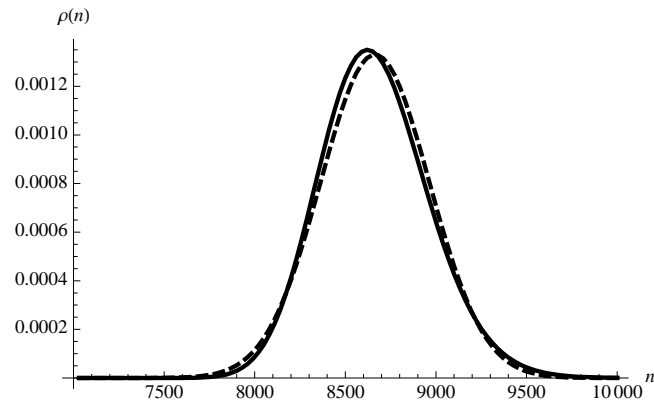
Fig. 21. Noncondensate particle number distribution function for $N = 10000$ atoms in a box calculated via the FFT technique in accord with the Eq. (3.2) - (solid line) compared with the Gaussian distribution function in Eq. (3.10) - (dashed line).
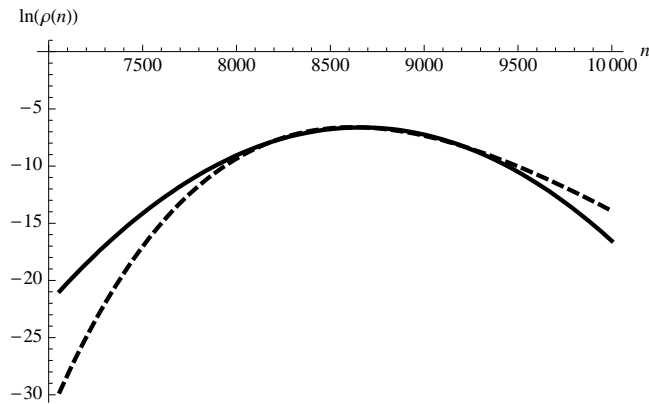
Fig. 22. Noncondensate particle number distribution function for $N = 10000$ atoms in a box calculated via the FFT technique in accord with the Eq. (3.2) - (solid line) compared with the Gaussian distribution function in Eq. (3.10) - (dashed line) in the logarithmic scale.
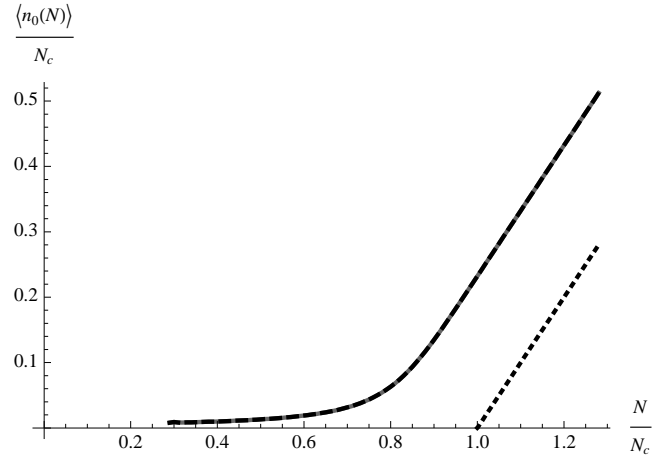
Fig. 23. Mean occupation number of condensed atoms for $N = 1000$ atoms in a box calculated via the FFT technique - (solid gray line) in accord with Eq. (3.4) compared with the same quantity calculated in the Gaussian approximation in Eq. (3.13) - (dashed black line) and mean field approximation $\bar{n}_0 \propto N - N_c$ in the thermodynamic limit - (black dotted line)
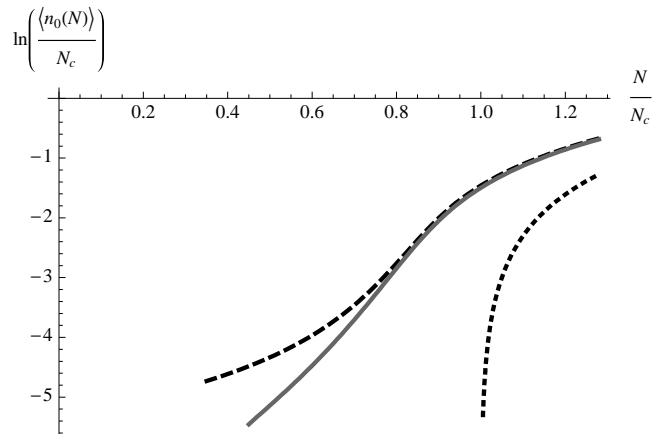
Fig. 24. Mean occupation number of condensed atoms for $N = 1000$ atoms in a box calculated via the FFT technique - (solid gray line) in accord with Eq. (3.4) compared with the the same quantity calculated in the Gaussian approximation in Eq. (3.13) -(dashed black line) and mean field approximation $\bar{n}_0 \propto N - N_c$ in the thermodynamic limit - (black dotted line) in the logarithmic scale.

$$\frac{\left\langle \left(n_0(N) - \langle n_0(N) \rangle \right)^3 \right\rangle}{N_c^{3/2}}$$
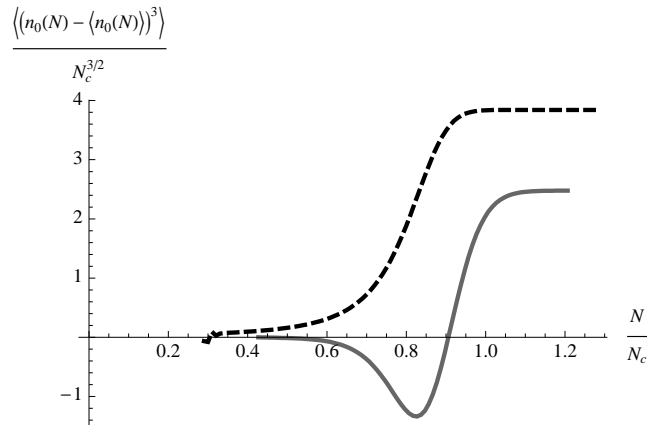
Fig. 25. Third central moment of condensed atoms for $N = 1000$ atoms in a box calculated via the FFT technique - (solid gray line) in accord with Eq. (3.7) compared with the same quantity calculated in the Gaussian approximation in Eq. (3.12) - (dashed black line).

corresponds to the non-Gaussian behavior of the distribution function at the wings. Higher moments will deviate much more. The latter can be seen in Fig. 25 for the case of the third moment, that has even qualitatively different structure. In Gaussian approximation, the distribution function is purely symmetric, which means that the third moment would have the same sign for all values of argument. The higher order cumulants turn out to be essentially non-zero, which is a distinctive feature of any non-Gaussian probability distribution.

Using the simple argument and consideration of the one-scale problem, one can apply the above formalism to a direct calculation of the asymptotic expression for the distribution function, which is done in the following Chapter IV. In the following discussion, I will analyze not only the Gaussian approximation for the distribution function, but each scale for each part of the distribution function corresponding to the high and low values of the argument.

CHAPTER IV

SADDLE-POINT METHOD FOR CONDENSED BOSE GASES

A.   Review of the saddle-point method for a condensed Bose gas in a harmonic trap

The saddle-point method is a very powerful technique in statistical physics, but its canonical form is not applicable in the case of a systems with condensate. As it is discussed in Appendices, the characteristic function has an infinite number of poles on the real positive half of z axis. The lowest order pole is at the point $z_1 = e^{\epsilon_1/T}$. Since we are integrating over the unit circle in the complex plane and the distance between the saddle point and the lowest pole can be infinitesimal, the traditional Gaussian approximation requires the vicinity of the saddle point to have no singularities. Following the approach introduced by Holthaus and Kalinowski [20, 27], I will give a solution to this problem by exempting the minimal energy contribution from the characteristic function treating it explicitly, and performing the Gauss integration as usual. As result, I will obtain an expression in terms of the hypergeometric functions, which leads to the parabolic cylinder functions. First, I will apply this technique to the problem of an ideal Bose gas in a harmonic trap, reviewing the solution in thermodynamic limit. I start with the grand canonical partition function:

$$\Xi(\beta, z) = \prod_{\nu=0}^{\infty} \frac{1}{1 - z \exp(-\beta\epsilon_\nu)}, \tag{4.1}$$

where ϵ_ν are single-particle energies, $\beta = 1/T$ (T is expressed in energy units) and $z = \exp(\beta\mu)$. The grand canonical partition function $\Xi(\beta, z)$ generates the canonical partition function $Z_N(\beta)$ by means of the expansion:

$$\Xi(\beta, z) = \sum_{N=0}^{\infty} z^N Z_N(\beta). \tag{4.2}$$

Then one can treat z as a complex variable and express $Z_N(\beta)$ as a contour integral using the Cauchy's theorem:

$$Z_N(\beta) = \frac{1}{2\pi i} \oint dz \frac{\Xi(\beta, z)}{z^{N+1}} = \frac{1}{2\pi i} \oint dz \exp(-F(z)), \qquad (4.3)$$

where the path of integration encircles the origin counterclockwise, and

$$F(z) = (N+1)\ln(z) + \ln \Xi(\beta, z) = (N+1)\ln(z) + \sum_{\nu=0}^{\infty} \ln\left(1 - z\exp(-\beta\epsilon_\nu)\right). \quad (4.4)$$

The usual definition for the saddle point $(z = z^*)$ requires the first derivative to be zero in this point

$$\left.\frac{dF}{dz}\right|_{z=z^*} = 0, \qquad (4.5)$$

which gives the following equation for z^*

$$N + 1 = \sum_{\nu=0}^{\infty} \frac{1}{\exp(\beta\epsilon_\nu/z^*(N)) - 1}. \qquad (4.6)$$

This is almost the grand canonical relation between particle number $N+1$ and the fugacity z_0. In the case of a harmonic trap (linear spectrum) [27] this equation can be solved in the continuum limit, which leads to the dilogarithm functions. In the canonical saddle-point method the Taylor expansion of the function $F(z)$ yields

$$F(z) \approx F(z^*) + \frac{1}{2}F''(z^*)(z - z^*)^2. \qquad (4.7)$$

Thus, performing the Gaussian integral, one can obtain:

$$Z_N(\beta) \approx \frac{\exp(-F(z^*(N)))}{\sqrt{-2\pi F''(z^*(N))}}. \qquad (4.8)$$

The canonical occupation number of the ground state, and its mean-square fluctuations, are obtained by differentiating the canonical partition function:

$$\bar{n}_0 = \frac{\partial Z_N(\beta)}{\partial(-\beta\epsilon_0)} = \frac{1}{Z_N(\beta)}\frac{1}{2\pi i}\oint dz \frac{\partial \Xi(\beta, z)}{\partial(-\beta\epsilon_0)}, \qquad (4.9)$$

$$\Delta n_0 = \frac{\partial^2 Z_N(\beta)}{\partial(-\beta\epsilon_0)^2} = -\bar{n}_0^2 + \frac{1}{Z_N(\beta)} \frac{1}{2\pi i} \oint dz \frac{\partial^2 \Xi(\beta, z)}{\partial(-\beta\epsilon_0)^2}. \tag{4.10}$$

The saddle-point approximation is then applied to the integrands of Eqs. (4.9) and (4.10). In the condensate region there is a substantial deviation of the saddle-point expressions from the "exact" numerical answer obtained from the exact recursion relation (2.36).

The reason of this inaccuracy is that in the condensate region, the saddle-point z_0 lies close to the singular point $z = e^{\beta\epsilon_0}$ of the function $F(z)$. As result, the approximation in Eq. (4.8) becomes invalid in the condensate region. To improve this method, it was proposed in Ref. [27] to treat the potentially dangerous term in (4.4) as it is, and represent $Z_N(\beta)$ as:

$$Z_N(\beta) = \frac{1}{2\pi i} \oint dz \frac{\exp(-F_1(z))}{1 - z \exp(-\beta\epsilon_0)}, \tag{4.11}$$

where

$$F_1(z) = (N+1)\ln(z) + \sum_{\nu=1}^{\infty} \ln\left(1 - z\exp(-\beta\epsilon_\nu)\right) \tag{4.12}$$

has no singularity at $z = e^{\beta\epsilon_0}$. If the point of singularity exists, it is shifted now to the next available pole, i.e. $z = e^{\beta\epsilon_1}$. Since $z^* < e^{\beta\epsilon_0}$, the saddle point is far away from the singularity point by the distance $e^{\beta\epsilon_1} - e^{\beta\epsilon_0} \approx \hbar\omega/T$, which makes the expansion (4.12) valid and safe for sufficiently large number of particles N. One can use the following expression for the integral in Eq. (4.11):

$$\frac{1}{2\pi i} \oint dz \frac{\exp\left[-f_1(z) - (\sigma - 1)\beta\epsilon_0\right]}{(1 - z\exp(-\beta\epsilon_0))^\sigma} \approx$$

$$\approx \frac{1}{\sqrt{2\pi}} \left(-f_1''(z^*)\right)^{(\sigma-1)/2} \exp\left(\beta\epsilon_0 - f_1(z^*) - \sigma + \eta^2/2 - \eta_1^2/4\right) D_{-\sigma}(\eta_1), \tag{4.13}$$

where $\eta = (\exp(\beta\epsilon_0) - z^*)\sqrt{-f_1''(z^*)}$, $\eta_1 = \eta - \sigma/\eta$, z^* is a saddle point of the

function,

$$f(z) = f_1(z) + (\sigma - 1)\beta\epsilon_0 + \sigma \ln(1 - z \exp(-\beta\epsilon_0)), \tag{4.14}$$

and $D_{-\sigma}(z)$ is a parabolic cylinder function. This function can be further written as a combination of the hypergeometric functions as

$$D_s(z) = 2^{s/2} e^{-z^2/4} \sqrt{\pi} \left[\frac{{}_1F_1(-s/2, 1/2, z^2/2)}{\Gamma[(1-s)/2]} - \frac{\sqrt{2}z \cdot {}_1F_1((1-s)/2, 3/2, z^2/2)}{\Gamma[-s/2]} \right]. \tag{4.15}$$

Thus, the integration in Eq. (4.11) yields:

$$Z_N(\beta) = \frac{1}{2} \exp\left(\beta\epsilon_0 - F_1(z^*) - 1 + \eta^2/2\right) \mathrm{erfc}\left(\frac{\eta_1}{\sqrt{2}}\right), \tag{4.16}$$

where $\mathrm{erfc}(z) = 2/\sqrt{2} \int_z^\infty \exp(-t^2) dt$ is the complementary error function,

$$\eta = (\exp(\beta\epsilon_0) - z^*) \sqrt{-F_1''(z^*)}, \qquad \eta_1 = \eta - 1/\eta, \tag{4.17}$$

since in the case of a harmonic trap $\sigma = 1$. Calculations of the occupation number, variance, and higher moments deal with the integrals from derivatives of $\Xi(\beta, z)$ with respect to $-\beta\epsilon_0$. The refined saddle-point expressions for the first four central moments or cumulants are in remarkable agreement with the numerical results obtained from the exact recursion relation for an ideal gas in a harmonic trap.

B.   The development of the saddle-point method for a condensed Bose gas in a box

I express the characteristic function as the contour integral over the unit circle in the complex z-plane using the Cauchy's theorem for $z = e^{iu}$:

$$\rho(n) = \frac{1}{2\pi} \int_{-\pi}^{\pi} e^{-inu} \Theta_n(u) \, du = \frac{\Theta_0}{2\pi i} \oint_{|z|=1} dz \frac{\tilde{\Theta}(z)}{z^{n+1}} = \frac{1}{2\pi i} \oint_{|z|=1} dz \exp(-F(z)), \tag{4.18}$$

where the path of integration encircles the origin counterclockwise, and in the case of a box:

$$\Theta_0 = \prod_{\mathbf{k}\neq 0} (1 - 1/z_{\mathbf{k}}), \qquad \tilde{\Theta}(z) = \prod_{\mathbf{k}\neq 0} \frac{1}{1 - z/z_{\mathbf{k}}}, \tag{4.19}$$

$$F(z) = (n+1)\ln(z) + \ln\Theta(z) = (n+1)\ln(z) + \sum_{\mathbf{k}\neq 0} \ln\left(1 - z/z_{\mathbf{k}}\right). \tag{4.20}$$

The equation for the saddle point z^* is:

$$n + 1 = \sum_{\mathbf{k}\neq 0} \frac{1}{z_{\mathbf{k}}/z^*(n) - 1}. \tag{4.21}$$

As result, for the standard saddle-point approximation one can obtain:

$$\rho(n) \approx \frac{\exp(-F(z^*(n)))}{\sqrt{-2\pi F''(z^*(n))}}. \tag{4.22}$$

In fact, the deviation from the exact solution in the canonical saddle-point method for a box can only be seen in the condensate regime, and thus, for our purposes, (in the critical region), the approximation in Eq. (4.22) gives precise enough estimate. Nevertheless, the refined saddle-point method gives a much better accuracy. Hence, one should express the distribution function in the following way:

$$\rho(n) = \frac{\Theta_0}{2\pi i} \oint_{|z|=1} dz \frac{\exp(-F_1(z))}{1 - z/z_0}, \tag{4.23}$$

where the function

$$F_1(z) = (n+1)\ln(z) + \sum_{\mathbf{k}\neq 0,1} \ln\left(1 - z/z_{\mathbf{k}}\right), \tag{4.24}$$

has no singularity at $z = e^{\epsilon_1/T}$. If the point of singularity exists, it is shifted now to the next available pole, i.e. $z = e^{2\epsilon_1/T}$. Since $z^* < e^{\epsilon_1/T}$, the saddle point is far away from the singularity point by the distance $e^{2\epsilon_1/T} - e^{\epsilon_1/T} \approx N\epsilon_1/T$, which makes the expansion in Eq. (4.24) valid for sufficiently large number of particles N. Now I

employ the expression obtained in the previous section for the integral in Eq. (4.13). The corresponding degeneracy is $g_1 = \sigma = 6$ and, thus, one can express the resulting distribution function as:

$$\rho(n) = \frac{1}{\sqrt{2\pi}} \left(-F_1''(z^*(n))\right)^{5/2} \times$$

$$\times \exp\left(\epsilon_1/T - F_1(z^*(n)) - 6 + \eta^2(n)/2 - \eta_1^2(n)/4\right) D_{-6}(\eta_1(n)). \tag{4.25}$$

Using the above result, one can analyze the asymptotical behavior of the distribution function and estimate the leading term in the expansion. I return to the Eq. (4.21) for the saddle point definition. Let us consider a small n, so that $n << N$. The particular choice of the estimate is obvious. I would like to analyze the behavior far from the maximum value of the function, where it can be approximated by Gaussian function. In this case, expanding the right-hand-side of the Eq. (4.21) and implying that $z^*(n = 0) \approx 0$, $\delta z = z^* - 0 \approx (n+1)/f_1(0)$, where:

$$f_m(z) = \sum_{\mathbf{k} \neq 0} (z - z_{\mathbf{k}})^{-m}, \tag{4.26}$$

the saddle-point approximation yields the following result $\rho(n)|_{n<<N} \approx n^n$, or more accurately:

$$\rho(n)|_{n<<N} \propto n^n e^{(\ln f_1(0) + 1/2)n}. \tag{4.27}$$

Here all n's are properly normalized by the variance. Going further, one can obtain that the dependence in the vicinity of the maximal value is truly gaussian with the parameters $\bar{n}$ and Δ. In this case $\delta z = z^* - \bar{z} = \frac{\bar{z}\delta n}{\bar{z}^2 f_2(\bar{z}) + \bar{n}}$. Thus, performing the integration, one can obtain:

$$\rho(n \approx \bar{n}) \propto e^{-\frac{(n-\bar{n})^2}{f_2(\bar{z})\bar{z}^2 + \bar{n}}} \approx e^{-\frac{(n-\bar{n})^2}{\Delta^2}}, \tag{4.28}$$

where $\bar{z} = z(\bar{n})$. At large n, of the order of N, the value $z(N)$ is close to the pole at $z = e^{2\epsilon_1/T}$, which means, that the Gaussian function should decay fast enough from its maximum value. In other words, the width of the Gaussian function should be much smaller than the distance between the saddle point itself and the closest pole: $z(N) - z(n) << e^{2\epsilon_1/T} - z(N)$. Therefore, the allowed region for n is $N - n << \Delta$. In this case, one can expect the linear-exponentially decaying behavior, i. e.,

$\delta z = z(N) - z(n) \approx \frac{z(N)\delta n}{z^2(N)f_2(z(N))+N}$, and finally

$$\rho(n \approx N) \propto e^{-\ln(z(N))(N-n)} \propto e^{-3(N-n)/\Delta} \tag{4.29}$$

I intentionally dropped the pre-exponential factors, which depends on n, since I am considering the leading order asymptotical behavior of the distribution function. The universality of the asymptotics is really surprising, since the proper scaled distribution functions for the different size of the traps have not only the same shape, but are almost identical, which means, that there are only two real macroscopical scales of the distibution function. First scale is its maximum value at thermal mean occupation number $\bar{n}$. The second one is the characteristic width scale, which is essentially the variance, calculated in the thermal approximation. Those similarities imply the universality in the description of the statistical moments, the same way it was done for the distribution function in Chapter III. Many efforts were done to analyse the closed form of universal function such as $n_0(N)$ (see Chapter III, Section C) and higher moments, but this result will not be discuss in the present work.

C. Comparison with the numerical results

In this section, I present the comparison of the obtained results with the numerical simulations. I will compare the refined saddle point approximation results for the

Fig. 26. Canonical ensemble distribution function in the vicinity of its maximum as a function of the number of noncondensed particles in a box with $N = 10000$ atoms. Dashed and solid lines are obtained by the numerical calculation of discrete Fourier summation in Eq. (3.2) for an ideal gas and refined saddle–point method in Eq. (4.28), respectively.

asymptotical behavior of the distribution function and the result of applying the FFT technique in Eq. (3.2). It is worth noting that I am not using the saddle-point approximation for calculation of the condensate fluctuations, like it was done in the case of a harmonic trap. According to the asymptotic formulas in Eqs. (4.27)-(4.29), one can separate the whole region of the distribution function by three parts.

The contribution around the mean occupation number of the condensate $\bar{n}$ is Gaussian, with a relatively good accuracy (see Eq. (4.28) and Fig. 26). It has a little shift in its maximum value due to the fact that one used the finite summation over momenta when evaluating the thermal mean occupation number and its variance instead of performing the infinite summation.

A similar analysis can be performed in the evaluation of the contributions at the wings. I found that, in the lower-N region, the behavior is almost exponential, which means that its logarithm is a linear function of N (see Eq. (4.27) and Fig.27). It

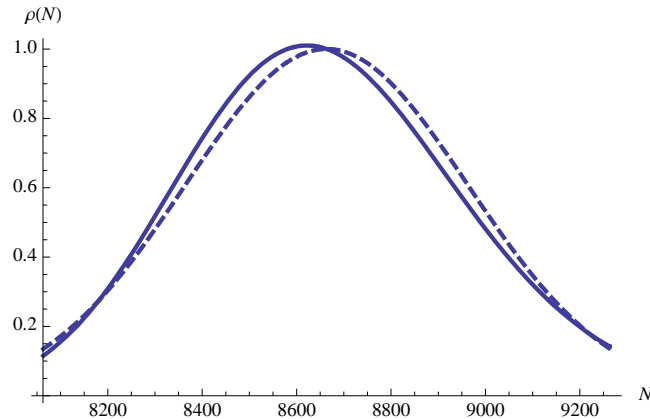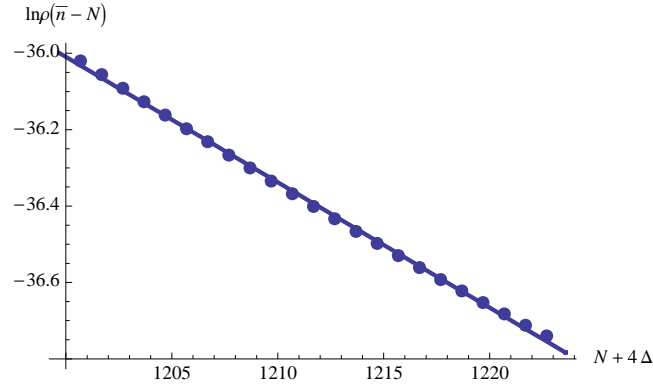Fig. 27. Logarithm of the canonical ensemble distribution function in the region of small n as a function of a number of noncondensed particles in a box with $N = 10000$ atoms. Dashed and solid lines are obtained by the numerical calculation of discrete Fourier summation in Eq. (3.2) for an ideal gas and refined saddle-point method in Eq. (4.27), respectively.

follows from the fact that $\log(n)$ term in the exponent is a smooth function, almost a constant if the argument N is varying slowly. The distribution function for the small N is plotted in the inverse direction from large N to small N, starting from 4Δ distance from the maximum value $\bar{n}$.

Similarly, one can consider the large N region. Here, one can see the exponential decay as well, but with a more smooth behavior (see Eq. (4.29) and Fig.28).

In conclusion, the saddle point method, which is truly very powerful approximation method in theoretical physics, leads to the simple analytical formulas for the BEC fluctuations in the different regions of the parameters.
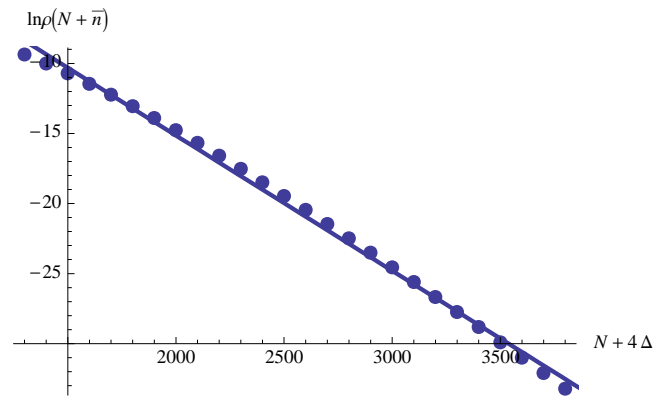
Fig. 28. Logarithm of the canonical ensemble distribution function in the region where n is of the order of N as a function of a number of noncondensed particles in a box with $N = 10000$ atoms. Dashed and solid lines are obtained by the numerical calculation of discrete Fourier summation in Eq. (3.2) for an ideal gas and refined saddle-point method in Eq. (4.29), respectively.

CHAPTER V

CONCLUSIONS AND DISCUSSIONS

A.   What is next: from ideal towards weakly interacting Bose gas

The presented above analysis of the condensate fluctuations in an ideal Bose gas in a box, in particular, the canonical ensemble quasiparticle method, can be extended to more realistic models of Bose-Einstein condensate in a dilute gases which include interaction between atoms. The analytical formulas for the characteristic function and all cumulants are the generalizations of the expressions obtained for an ideal gas. Here I do not discuss the results in details, and only outline some of them.

The ground state occupation statistics is not Gaussian even in the thermodynamic limit. The effect of Bogoliubov coupling reveals the suppression of the ground-state occupation fluctuations, first found in [21, 33] and governed by a pair-correlation, squeezing mechanism. There is a crossover between an ideal and weakly interacting Bose gas, which can be described in a very elegant way, using the asymptotical expansion of the occupation statistics with respect to the interaction strength parameter. The pair correlation mechanism is a consequence of two-mode squeezing due to Bogoliubov coupling between $\mathbf{k}$ and $-\mathbf{k}$ modes. Thus, the fact that the dispersion of the condensate fluctuations in the interacting Bose gas is $1/2$ of that in an ideal Bose gas is not an accident.

The effect of suppression of the condensate fluctuations at low temperatures $(T << T_c)$ can be deduced from the asymptotic expansion of the properly normalized first four central moments of the ground state occupation statistics via the solution of the non-linear self-consistency equation for the mean ground state occupation number. These asymptotics are close to that, obtained from the cumulant analysis in [21]

similar to the formulas for an ideal gas in Eq. (2.19). The expressions presented below were obtained in the framework of the multinomial expansion (see Chapter II, Section E), taking into account modifications originated from the effect of weak interaction via the Bogoliubov spectrum and squeezed states. Thus, using explicitly the particle conserving formalism I found the following formulas for the mean value and its variance:

$$\frac{\bar{n}_0}{N} = 1 - \frac{1}{2}\frac{s_2\alpha^2}{N}\left(1 + \frac{v_2(T)}{\alpha^2}\right), \tag{5.1}$$

$$\mu_2 = s_2\alpha^2\left(1 + \frac{2v_2(T)}{\alpha^2}\right), \tag{5.2}$$

where

$$s_j = \sum_{\mathbf{k}\neq 0,\ (\mathbf{k},-\mathbf{k})} \frac{1}{\mathbf{k}^{2j}}, \tag{5.3}$$

$$v_j(T) = \sum_{\mathbf{k}\neq 0,\ (\mathbf{k},-\mathbf{k})} \mathbf{k}^{2j}\exp(-j\epsilon_1\mathbf{k}^2/T), \tag{5.4}$$

$$\alpha = \frac{U_0 N}{\epsilon_1 L^3}. \tag{5.5}$$

The summation in Eq. (5.3) is running over all different pairs of $(\mathbf{k}, -\mathbf{k})$ modes, $U_0 = \frac{4\pi\hbar^2 a}{m}$ is an interaction strength, proportional to the s-wave scattering length a. The results in Eqs. (5.1) and (5.2) are valid when $v_2 << \alpha^2$, which follows from the condition $T << \epsilon_1$ and prove that in the zero temperature limit the condensate fluctuations are suppressed by the factor proportional to the square of the interaction strength parameter and tend to zero for all moments except for the ground state mean occupation number.

One can also obtain the crossover between fluctuations in an ideal and weakly interacting Bose gases. In particular, I obtain the high temperature asymptotics $(T >> T_c)$ for the initial moments of the BEC fluctuations of any order. Below I

present these formulas in term of relations between the condensate fluctuations in the weakly interacting Bose gas (left-hand-side with "int" subscript) to the condensate fluctuations in an ideal Bose gas (right-hand-side, without subscripts). The solution of the nonlinear self-consistency equation for the mean ground state occupation number is:

$$\langle n_{0_{int}}\rangle = \frac{\langle n_0 \rangle}{1 - \xi \left(\frac{\langle n^2 \rangle - \langle n \rangle \langle n_T \rangle}{N} + \langle n_T \rangle - \langle n \rangle \right)}. \tag{5.6}$$

The initial (noncentered) moments of the number of the noncondensed atoms are:

$$\langle n^p_{int}\rangle = \frac{1 - \xi \left(\frac{\langle n^2 \rangle}{N} - \langle n \rangle + \frac{\langle n^{p+1} \rangle}{\langle n^p \rangle} \langle \frac{n_0}{N} \rangle \right)}{1 - \xi \frac{\langle (n - \langle n \rangle)^2 \rangle}{N}} \langle n^p \rangle, \tag{5.7}$$

where $\langle n_T \rangle = \sum_{\mathbf{k} \neq 0} \left(\exp(\epsilon_{\mathbf{k}}/T) - 1 \right)^{-1}$ is the usual Bose-Einstein occupation number and $\xi = \epsilon_1 \alpha / T$. It is easy to check that in the limiting case of vanishing interaction strength the fluctuations become the same as they were in an ideal gas. The condition of an applicability of the presented above high temperature asymptotical expansions is:

$$\frac{T}{T_c} >> 2\frac{a}{L}(\zeta(3/2))^{2/3} N^{1/3} \bar{n}_0 \tag{5.8}$$

where I explicitly used the expression for the interaction strength in term of the s-wave scattering length, $U_0 = 4\pi\hbar^2 a/m$. This condition is satisfied for a wide range of parameters in real experiments [12–14] and thus can be used to illuminate the crossover between the fluctuations in the ideal and weakly interacting Bose gases. I would like to emphasize that the above crossover relations, i.e. the high temperature asymptotics, were derived using the particle-number constraint, the canonical ensemble quasiparticle formalism, and the multinomial expansion.

B.   Summary of the main results

The statistics of the BEC fluctuations in an ideal gas in a box in the thermodynamic limit and in the systems with a finite number of particles is essentially the statistics of the sum of the noncondensed quasiparticles $n_{\mathbf{k}}$, $n_0 = N - \sum_{\mathbf{k} \neq 0} n_{\mathbf{k}}$. This statistics is very different from the standard thermodynamics fluctuations and is strongly non-Gaussian. It justified it by explicit calculation of the cumulants and central moment of all orders in the properly reduced many-body Fock space in this work.

In Chapter I, Section A, I outlined the phenomenon of Bose-Einstein condensation and the concept of the condensate wave function as a coherent macroscopic order parameter of the BEC second order phase transition, first introduced by Landau in the theory of superfluidity. I briefly discussed the parameters of the recent BEC experiments such as the parameters of the trapping potentials and laser beams as well as the methods of trapping and cooling.

In Section B, I presented the main theoretical concepts in analyzing the problem of BEC fluctuations and mesoscopic effects. I started with the classical formulation of the problem and discussed two major steps in the development of the microscopic theory due to Bogoliubov and Belyaev. I compared the results obtained in the micro-canonical, canonical, and grand-canonical ensembles and the exact recursion relation for the distribution function of the condensed atoms which is useful for numerical computation of the statistics of BEC. I briefly outlined the dynamical master-equation approach and analogy with the laser transition. I discussed also the integral representation of the distribution function in terms of the generalized zeta function which is an alternative way of applying the canonical quasiparticles formalism, presented in Chapter II.

In Chapter I, I presented mostly the known results and made an introduction to

the subject of the present work.

The rest of the chapters are mainly devoted to the presentation of the new results.

In Chapter II, Section A, I formulated the known canonical quasiparticle formalism, which allows one to analyze the condensate fluctuations as being complimentary to the independent fluctuations of the noncondensate quasiparticles.

In Section B, I presented the characteristic function for the ground state occupation number of an ideal Bose gas and its connection to the distribution function of the noncondensed atoms in a trap. Then I discussed the problem of the mesoscopic effects, which were not taken into account in the previous works utilizing the Maxwell's demon ensemble approximation [20, 21, 28, 34].

In Section C, I presented the weighted distribution function Eq.(2.22), which was constructed via appropriate implementation of the particle-number constraint and, therefore, allows one to avoid an incorrect growth of the statistical moments at $T > T_c$ in Eq. (2.23).

In Section D, I described a proper way of the evaluation of the sums and products in the momentum space using the symmetry of the boundary conditions. In particular, I calculated in this way the characteristic function in Eq. (2.29).

In Section E, Eq. (2.35) I presented one of the main results of the work, namely, I derived the closed form expression for the distribution function of the noncondensed atoms in an ideal Bose gas in a box using the multinomial expansion. The analytical formulas for the moments presented in Eq. (2.23) with the distribution function in Eq. (2.35) explicitly obey the particle number constraint and are in the good agreement with the exact recursion relation in Eq. (2.36) for an ideal gas [20]. The latter was shown in Section F, where I plotted the temperature scaled fluctuations in Figs. 2-6 calculated via the multinomial expansion and compared them with the thermodynamic limit expressions [21]. The low-temperature asymptotic formula (2.40)

coincides with the formula obtained previously in [21]. In contrast with that, the high temperature asymptotics, which were infinitely large in Eq. (2.41) for all moments starting from the variance in [21], in this work is finite and consistent with the grand-canonical ensemble expression for an ideal gas in Eq. (2.45), that is true high temperature asymptotics.

In Chapter III, Section A, I presented the detailed analysis of the distribution function for the canonical ensemble statistics within the fixed temperature approach. It essentially lowers the number of the operations involved in the evaluation of the Fourier integrals for the sufficiently large but finite number of particles, and is true even for the thermodynamic limit.

In Section B the technique of the Fast Fourier Transformation (FFT) was used in the numerical computation of the distribution function of the noncondensed atoms and its moments Eq. (3.2). I computed the macroscopic order parameter in Eq. (3.3) and the ground state occupation number in Eq. (3.4). I plotted both of them as the functions of the number of particles in a trap in Figs. 8 and 9, respectively. I compared the obtained above expressions with the mean field approximation, of the Landau theory of phase transitions [4, 5] which is valid in the thermodynamic limit. The variance of the macroscopic order parameter in Eq. (3.5) is plotted as the function of the number of particles in Fig. 11. The variance of the ground state occupation number in Eq. (3.6) is plotted in Fig. 12. The central third moment in Eq. (3.7) is plotted as a function of the number of particles in Figs. 14 and 15. The central fourth moment in Eq. (3.8) is plotted in Figs. 16 and 17. I explicitly checked that the mesoscopic fluctuations tend to the thermodynamic limit results when $N \to \infty$, $V \to \infty$, and $N/V = \text{const}$.

In Section C, I discussed the self-similarities in the BEC fluctuations. I introduced the universal scale of the distribution function and showed that in the lowest

order approximation in the region around the maximum, $|N - \bar{N}| << N$, the properly scaled distribution functions are described by a numerical curve (see Figs. 18 and 19). The proper scale is the variance of ground state occupation number calculated in the thermal approximation in Eq. (3.11). I checked that if the distribution function was a pure Gaussian function as in Eq. (3.10) and Fig. 21, the fluctuations behave wrongly almost for all values of the argument N, starting from the mean occupation number of the ground state in Figs. 23 and 24 for small N, and have qualitatively wrong behavior for higher moments, Fig. 25.

In Chapter IV, I analyzed the asymptotical behavior of the ground state occupation statistics in the framework of the refined saddle point approximation. In Section A I reviewed the saddle-point method for a Bose gas in a harmonic trap following [27].

In Section B, I applied the presented formalism to the condensed Bose gas in a box. In both cases it leads to the parabolic cylinder functions as a basis for the cumulants and other statistical moments. The complications of the present calculations for an ideal gas in a box compared to the case of the harmonic trap originate from the degeneracies and symmetries of the boundaries.

In Section C, I compared the obtained in Section B asymptotic formulas for the different regions of the argument, Eqs. (4.27) - (4.29) with the results calculated via the FFT method, discussed in Section B. The resulting curves are presented in Figs. 26-28. These asymptotic formulas extract the natural scale of the distribution function, which agrees with the conclusion of Chapter III.

In the appendices, I presented the detailed derivation and relations between the characteristic and distribution function (A.4) and the initial statistical moments of the ground state occupation number (B.5) via the residue technique. Also I presented the detailed derivation of the multinomial expansion approach for the condensate

statistics and the closed form expression for the distribution function of the non-condensed atoms in Eq. (C.9).

As it was discussed in Section A of the present chapter, the next step in the analysis of BEC statistics will be the computation of the mesoscopic effects in a weakly interacting Bose gas by means of the Bogoliubov approximation and by means of the advanced diagram methods which should also include explicitly the conservation of the number of particles in a trap. The preliminary analysis indicates the suppression of the condensate fluctuations at high temperatures and their enhancement at low temperatures as compared to the case of an ideal gas. The work in this direction is in process and will be presented elsewhere.

Clearly, the mesoscopic effects in the Bose-Einstein condensate fluctuations constitute an important class of problems in the many-body physics.

BIBLIOGRAPHY

[1] A. Einstein, Sitzungsberichte der preussischen Akademie der Wissenschaften, XXII. Gesamtsitzung **10**, 261 (1924).

[2] A. Einstein, Sitzungsberichte der preussischen Akademie der Wissenschaften, XXII, I. Sitzung der physikalisch-mathematischen Klasse **8**, 3 (1925).

[3] S. N. Bose, Z. Phys. **26**, 178 (1924).

[4] L. Landau and E. M. Lifshitz, *Statistical Physics, Part 1* (Pergamon, Oxford, 1969).

[5] E. M. Lifshitz and L. P. Pitaevskii, *Statistical Physics, Part 2* (Pergamon, Oxford, 1981).

[6] A. Z. Patashinsky and V. L. Pokrovsky, Sov. Phys. JETP **37**, 733 (1974).

[7] P. Pitaevskii and S. Stringari, Rev. Mod. Phys. **71**, 463 (1999).

[8] H. Shi and A. Griffin, Phys. Rep. **304**, 1 (1998).

[9] M. Anderson, J. Ensher, M. Matthews, C. Wieman, and E. Cornell, Science **269**, 198 (1995).

[10] K. B. Davis, M.-O. Mewes, M. R. Andrews, N. J. van Druten, D. S. Durfee, D. M. Kurn, and W. Ketterle, Phys. Rev. Lett. **75**, 3969 (1995).

[11] C. C. Bradley, C. A. Sackett, J. J. Tollett, and R. G. Hulet, Phys. Rev. Lett. **75**, 1687 (1995).

[12] A. Leggett, Rev. Mod. Phys. **73**, 307 (2001).

[13] C.-S. Chuu, F. Schreck, T. P. Meyrath, J. L. Hanssen, G. N. Price, and M. G. Raizen, Phys. Rev. Lett. **95**, 260403 (2005).

[14] A. M. Dudarev, M. G. Raizen, and Q. Niu, Phys. Rev. Lett. **98**, 063001 (2007).

[15] T. P. Meyrath, F. Schreck, J. L. Hanssen, C.-S. Chuu, and M. G. Raizen, Phys. Rev. A **71**, 041604 (2005).

[16] C. D. J. Sinclair, E. A. Curtis, I. L. Garcia, J. A. Retter, B. V. Hall, S. Eriksson, B. E. Sauer, and E. A. Hinds, Phys. Rev. A **72**, 031603(R) (2005).

[17] Y.-J. Wang, D. Z. Anderson, V. M. Bright, E. A. Cornell, Q. Diot, T. Kishimoto, M. Prentiss, R. A. Saravanan, S. R. Segal, and S. Wu, Phys. Rev. Lett. **94**, 090405 (2005).

[18] G.-B. Jo, Y. Shin, S. Will, T. A. Pasquini, M. Saba, W. Ketterle, and D. E. Pritchard, Phys. Rev. Lett. **98**, 030407 (2007).

[19] S. Stringari, Phys. Rev. Lett. **86**, 4725 (2001).

[20] V. V. Kocharovsky, Vl. V. Kocharovsky, M. Holthaus, C. H. R. Ooi, A. Svidzinsky, W. Ketterle, and M. O. Scully, *Advances in Atomic, Molecular and Optical Physics*, vol. 53 (Elsevier Inc., Amsterdam, 2006).

[21] V. V. Kocharovsky, Vl. V. Kocharovsky, and M. O. Scully, Phys. Rev. A **61**, 053606 (2000).

[22] A. A. Abrikosov, L. P. Gorkov, and I. E. Dzyaloshinskii, *Methods of Quantum Field Theory in Statistical Physics* (Prentice-Hall, Englewood Cliffs, NJ, 1963).

[23] A. L. Fetter and J. D. Walecka, *Quantum Theory of Many-Particle Systems* (McGraw-Hill, San Francisco, 1971).

[24] B. C. Crooker, B. Hebral, E. N. Smith, Y. Takano, and J. D. Reppy, Phys. Rev. Lett. **51**, 666 (1983).

[25] M. H. W. Chan, K. I. Blum, S. Q. Murphy, G. K. S. Wong, and J. D. Reppy, Phys. Rev. Lett. **61**, 1950 (1988).

[26] P. A. Crowell, F. W. V. Keuls, and J. D. Reppy, Phys. Rev. Lett. **75**, 1106 (1995).

[27] M. Holthaus and E. Kalinowski, Ann. Phys. (N.Y.) **276**, 321 (1999).

[28] V. V. Kocharovsky, M. O. Scully, S.-Y. Zhu, and S. Zubairy, Phys. Rev. A **61**, 23609 (2000).

[29] M. Abramowitz and I. A. Stegun, *Handbook of Mathematical Functions* (Dover, New York, 1972).

[30] M. Girardeau and R. Arnowitt, Phys. Rev. **113**, 755 (1959).

[31] M. D. Girardeau, Phys. Rev. A **58**, 775 (1998).

[32] N. L. Balazs and T. Bergeman, Phys. Rev. A **58**, 2359 (1998).

[33] V. V. Kocharovsky, Vl. V. Kocharovsky, and M. O. Scully, Phys. Rev. Lett. **84**, 11 (2000).

[34] S. Grossmann and M. Holthaus, Optics Express **1**, 262 (1997).

APPENDIX A

DERIVATION OF THE ANALYTICAL FORMULAS FOR THE DISTRIBUTION
FUNCTION OF THE TOTAL NUMBER OF NONCONDENSED ATOMS IN AN
IDEAL GAS. METHOD OF THE CHARACTERISTIC FUNCTION AND
RESIDUES

I start with the defined in Chapter II distribution function in Eq. (2.8), written
as a Fourier integral from the characteristic function:

$$\rho\left(n\right) = \frac{1}{2\pi} \int_{-\pi}^{\pi} e^{-inu} \Theta_n(u)\, du. \tag{A.1}$$

Making the transformation of variable $z = e^{iu}$ in Eq. (A.1), one will obtain the
contour integral in the complex plane z, where the contour encircles the origin in the
counterclockwise direction:

$$\rho(n) = \frac{1}{2\pi i} \oint_{|z|=1} \frac{\Theta\left(z\right)}{z^{n+1}}\, dz = \frac{1}{2\pi i} \oint_{|z|=1} \frac{1}{z^{n+1}} \prod_{\mathbf{k}\neq 0} \frac{z_{\mathbf{k}} - 1}{z_{\mathbf{k}} - z}\, dz, \tag{A.2}$$

where $\Theta(z) = \Theta_n(u)$ with $z = e^{iu}$. The integrand in Eq.(A.2) has an infinite number
of poles at the positions $z = z_{\mathbf{k}}$ outside the contour, and the pole of the order of $n+1$
at the origin $z = 0$. The order of the each external pole is equal to the degeneracy of
of the $\mathbf{k}$ mode, i.e. $g_{\mathbf{k}} = 6, 8, 12, 24, 48$. Therefore, the integration can be performed
in two different ways.

First way is to sum up contributions from the residues in external poles. It is
convenient if the number of particles is sufficiently large ($N >> 48$). In this case the
highest derivative, to be calculated is of the order of 47 and it does not depend on

the particle number. The result of this calculation yields:

$$\rho(n) = \sum_{\mathbf{p}\neq 0} \operatorname*{res}_{z=z_{\mathbf{p}}} \frac{\Theta(z)}{z^{n+1}} = \sum_{\mathbf{p}\neq 0} \frac{1}{(g_{\mathbf{p}}-1)!} \frac{d^{g_p-1}}{dz^{g_p-1}} \left(\frac{\Theta(z)}{z^{n+1}} (z-z_{\mathbf{p}})^{g_p} \right) \Big|_{z=z_{\mathbf{p}}}, \qquad (A.3)$$

where an index $\mathbf{p}$ runs over different energy levels $\epsilon_{\mathbf{k}}$. Another way of calculation is to compute the $n+1$-st order residue at the origin. It looks more complicated in the sense of calculation higher order derivatives for large enough number of particles, but nevertheless I will present this result, since it leads to the closed form analytical expression for the distribution function useful in the analysis. Thus, one can find:

$$\rho(n) = \operatorname*{res}_{z=0} \frac{\Theta(z)}{z^{n+1}} = \frac{1}{n!} \frac{d^n}{dz^n} \Theta(z) \Big|_{z=0}, \qquad (A.4)$$

which is exactly the n-th coefficient in the Taylor expansion of the characteristic function about the point $z = 0$.

APPENDIX B

INITIAL (NONCENTERED) MOMENTS

In this section I apply the result in Eq. (A.4) to obtain the closed form expressions for the noncentered moments of the distribution function following the same path as was used for the calculation the distribution function itself. The advantage of using the zero-residue calculation is that one can perform explicitly the summation over n first, and then calculate the residue. This is true for the moments of any order. To see that I start with the lowest order moment - the zeroth order which is nothing but the normalization factor. The general expression for the initial moments is the following:

$$\alpha_m \equiv \langle n^m \rangle = \sum_{n=0}^{N} n^m \rho(n). \tag{B.1}$$

The integral expression for the normalization yields:

$$\alpha_0 \equiv \langle \theta(N - n) \rangle = \frac{1}{2\pi i} \oint_{|z|=1} \Theta(z) \sum_{n=0}^{N} \frac{1}{z^{n+1}}. \tag{B.2}$$

Performing the summation over n, using the geometric series, one obtains:

$$\sum_{n=0}^{N} \frac{1}{z^{n+1}} = \frac{1 - z^{N+1}}{z^{N+1}(1 - z)}. \tag{B.3}$$

Next step is to perform the contour integration with the pre-factor in Eq. (B.3) by evaluating the residue at the origin. The order of residue after the summation over n is $N + 1$. The point $z = 1$ in the denominator is a regular point, since there is a finite limit at $z \to 1$. Therefore, the resulting expression for the zeroth initial moment is:

$$\alpha_0 \equiv \langle \theta(N - n) \rangle = \frac{1}{2\pi i} \oint_{|z|=1} \Theta(z) \frac{1 - z^{N+1}}{z^{N+1}(1 - z)} = \operatorname*{res}_{z=0} \frac{1 - z^{N+1}}{z^{N+1}(1 - z)} \Theta(z) =$$

$$= \frac{1}{N!} \frac{d^N}{dz^N} \left(\frac{1 - z^{N+1}}{1 - z} \Theta(z) \right) \Big|_{z=0}. \tag{B.4}$$

All the higher moments can be written as a derivatives from the zeroth order $n^m = \left(-z\frac{d}{dz}\right)^m z^{-n}$, thus one can express the pre-factor of any moment in terms of the pre-factor of the zeroth order moment in Eq. (B.3). Therefore, for any noncentered moment of the distribution function one can write:

$$\alpha_m = \frac{1}{N!} \frac{d^N}{dz^N} \left(F_m(z) z^{N+1} \Theta(z) \right) \Big|_{z=0}, \tag{B.5}$$

where the general form of the pre-factor is:

$$F_m(z) = \left(-z\frac{d}{dz}\right)^m \frac{1 - z^{N+1}}{z^{N+1}(1 - z)}. \tag{B.6}$$

APPENDIX C

THE MULTINOMIAL EXPANSION

Let us go back to the characteristic function of the total number of noncondensed atoms. It can be written in different ways:

$$\Theta\left(z\right) = \prod_{\mathbf{k}\neq 0} \frac{z_{\mathbf{k}} - 1}{z_{\mathbf{k}} - z} = \prod_{\mathbf{k}\neq 0} \frac{z_{\mathbf{k}} - 1}{z_{\mathbf{k}}} \prod_{\mathbf{k}\neq 0} \frac{1}{1 - z/z_{\mathbf{k}}} = \Theta_0 \exp\left(-\sum_{\mathbf{k}\neq 0} \ln(1 - z/z_{\mathbf{k}})\right),$$

(C.1)

where $\Theta_0 \equiv \Theta(z = 0) = \prod_{\mathbf{k}\neq 0} \frac{z_{\mathbf{k}}-1}{z_{\mathbf{k}}}$ - the characteristic function at zero fugacity z. Now I employ the Taylor expansion of the logarithm under the summation about the point $z = 0$, using the fact, that $|z| < |z_{\mathbf{k}}|$, thus:

$$\ln(1 - z/z_{\mathbf{k}}) = -(z/z_{\mathbf{k}}) - \frac{(z/z_{\mathbf{k}})^2}{2} - \frac{(z/z_{\mathbf{k}})^3}{3} - \ldots = -\sum_{m=1}^{\infty} \frac{1}{m}\left(\frac{z}{z_{\mathbf{k}}}\right)^m.$$

(C.2)

One can rewrite (C.1), as following:

$$\Theta(z) = \Theta_0 \exp\left(\sum_{\mathbf{k}\neq 0}\sum_{m=1}^{\infty} \frac{1}{m}\left(\frac{z}{z_{\mathbf{k}}}\right)^m\right).$$

(C.3)

Changing the order of summation and defining $f_m(z) \equiv \sum_{\mathbf{k}\neq 0} (z - z_{\mathbf{k}})^{-m}$ and $f_m(0) \equiv f_m$, one can obtain:

$$\Theta(z) = \Theta_0 \exp\left(\sum_{m=1}^{\infty} f_m z^m\right).$$

(C.4)

Comparison of Eq. (C.4) with the distribution function in Eq. (A.4) allows one to conclude, that $\rho(n)$is nothing else but the Taylor coefficient of the z^n term, since all the other terms are zero. All terms of the lower orders vanish because of the higher order of the derivative, and all the higher order terms will be cancelled, because we have to set $z = 0$ in the end. Therefore, one can transform the expression for the characteristic function by replacing the infinite sum in the exponential power by

the finite, with the upper limit of N. I will leave the infinite sum, instead of the finite sum for the purpose of the more convenient definition, as will be explained later. Expanding the exponent in Taylor series with respect to z we are left with the following expression for the distribution function:

$$\rho(n) = \frac{\Theta_0}{n!} \frac{d^n}{dz^n} \left(\sum_{r=0}^{\infty} \frac{1}{r!} \left(\sum_{m=1}^{\infty} f_m z^m \right)^r \right) \Big|_{z=0}. \tag{C.5}$$

One can now employ the wonderful properties of the multinomial coefficients which are defined by the following formula [29]:

$$\left(\sum_{m=1}^{\infty} f_m z^m \right)^r \equiv r! \sum_{n=r}^{\infty} \frac{z^n}{n!} \sum (n; a_1, a_2, a_3..., a_n)^* f_1^{a_1} f_2^{a_2} f_3^{a_3} ... f_n^{a_n}, \tag{C.6}$$

summed over $a_1 + a_2 + a_3 + ... + a_n = r$ and $a_1 + 2a_2 + 3a_3 + .. + na_n = n$, where the multinomial coefficients have the following closed form expression:

$$(n; a_1, a_2, a_3..., a_n)^* = n!/1^{a_1} a_1! 2^{a_2} a_2! 3^{a_3} a_3! ... n^{a_n} n! \tag{C.7}$$

with the same restricted summation $a_1 + 2a_2 + 3a_3 + .. + na_n = n$. The meaning of these coefficients is the number of permutations of $n = a_1 + 2a_2 + 3a_3 + .. + na_n$ symbols composed of a_k cycles of length k for $k = 1, 2, 3, ..., n$. The useful property of the multinomial coefficients which connects them to the Stirling numbers of the first kind is $\sum (n; a_1, a_2, a_3..., a_n)^* = (-1)^{n-m} S_n^{(m)}$, summed over $a_1 + a_2 + a_3 + ... + a_n = m$ and $a_1 + 2a_2 + 3a_3 + .. + na_n = n$.

One can apply the expression (C.6) to obtain the distribution function:

$$\rho(n) = \frac{\Theta_0}{n!} \frac{d^n}{dz^n} \left(\sum_{r=0}^{\infty} \sum_{n=r}^{\infty} \frac{z^n}{n!} \sum (n; a_1, a_2, ..., a_n)^* f_1^{a_1} f_2^{a_2} ... f_n^{a_n} \right) \Big|_{z=0} \tag{C.8}$$

Now, changing the summation order and employing the discussed above conclusion, that n-th derivative is non zero only for the n-th term in the expansion, the result

can be written as:

$$\rho(n) = \frac{\Theta_0}{n!} \sum_{m=0}^{n} \sum_{\begin{pmatrix} a_1 + a_2 + ... + a_n = m \\ a_1 + 2a_2 + ... + na_n = n \end{pmatrix}} (n, a_1, a_2, ..., a_n)^* \prod_{j=1}^{n} f_j^{a_j}. \qquad \text{(C.9)}$$

The latter formula does not look very simple from the first sight. Nevertheless, it is very useful and, in particular, provides a convenient basis for the study of the limiting cases and asymptotical behavior, which are discussed in details in Section C of the Chapter II.

VITA

Konstantin Dorfman was born in Gorky, USSR. In September 2002, he entered Nizhny Novgorod State University and received his Bachelor of Science in physics in June 2006. In August 2006, he entered Texas A&M University and completed the requirements for the Master of Science degree in physics in August 2008. He may be reached at Department of Physics, Texas A&M University, College Station, Texas, 77843-4242.

The typist for this thesis was Konstantin Dorfman.